Review Article

Zeshan Abbas, Lun Zhao*, Jianxiong Deng, Shicheng Wang, and Wanlu Hong

Advances in ultrasonic welding of lightweight alloys: A review

https://doi.org/10.1515/htmp-2022-0298
received June 04, 2023; accepted October 30, 2023

Abstract: The lightweight alloy sheet materials have been widely used in industries such as automobiles, aviation, and aerospace. However, there are huge challenges in the structural joining process. Likewise, industries are probing new technologies and are rapidly adapting to more complex light alloy materials. The ultrasonic metal welding is a reliable solid-phase joining technology, which has incomparable development prospects in the high-strength joining of lightweight alloy sheet materials. This article summarizes the research progress of ultrasonic welding of aluminum alloy, magnesium alloy, and titanium alloy thin plates in recent years. The key features of this review article are the ultrasonic welding process, advantages, applications, and limitations. It introduces the welding process parameters to explore the breakthroughs for straightforward direction. Furthermore, to strengthen the phenomena, the current state of the ultrasonic welding of lightweight alloys and their future perspectives are also reflected.

Keywords: ultrasonic metal welding, lightweight alloys, welding process parameters, similar metals, dissimilar materials

1 Introduction

Contemporary, with the increasing demand for lightweight structures and light alloy sheet materials such as aluminum alloys, magnesium alloys [1,2], and titanium alloys have begun to be widely used in manufacturing industries [3]. The lightweight alloy sheet materials are increasingly used in automobiles, aviation, aerospace, sports, and many other applications as compared to conventional metals [4–8]. This is due to lower weight, specific stiffness, corrosion resistance, and high fatigue life compared to metals [9–12]. However, traditional spot welding has disadvantages such as gaps, cracks, and brittle compounds in light alloy connections which reduce the quality and reliability of the welded joints [13–18]. Therefore, it is imperative to develop new technologies for light alloy sheet material connection [19–23].

So far, magnesium, aluminum, and titanium are considered the light metals of the commercial sector and play a very strategic and important role in the development of the economy [24]. Similarly, their densities of 1.7, 2.7, and 4.5 $g \cdot cm^{-3}$ range from 19 to 56% of the densities of older structural metals such as iron (7.9) and copper (8.9) [25–29]. The aluminum has a low density which means it is light and easy to move from one place to another. Therefore, lightweight metals are the preferred choice when building airplanes for this powerful reason [30–33]. The aluminum material is also flexible and easy to use for lighter body shapes due to its lightweight properties. Therefore, this property makes it the perfect choice for manufacturing [4,34–36]. The aerospace industry relies heavily on alloy 7075 which is one of the highest strength lightweight aluminum alloys [37–42]. Likewise, alloy 2024 has a strength-to-weight ratio that is its outstanding feature and is used in many manufacturing parts that will be subjected to high levels of stress [43,44]. Additionally, alloy 7075 can be heat treated if needed for additive manufacturing. Literally, 6061 aluminum alloy sets the standard due to its specific properties such as light weight, medium to high strength, and economical material [30]. Likewise, some of the alloys were previously manufactured from aluminum alloy 6061. These metals had the problem of stress corrosion cracking while being subjected to the ultrasonic welding process [45]. However, the addition of chromium to these alloys provides them with corrosion resistance and increases manufacturing quality. The inherent strength of titanium metal will require a smaller portion of it, although titanium is about two-thirds times heavier than aluminum. In fact, studies need a fraction of the amount of titanium to get the same physical strength [6,46,47]. We would take aluminum after it has been ultrasonically welded. The

*** Corresponding author: Lun Zhao,** Institute of Ultrasonic Technology, Shenzhen Polytechnic University, Shenzhen, 518055, China,
e-mail: zhaolun@szpt.edu.cn, tel: +86 15112531731, fax: +86 75526731216
Zeshan Abbas, Jianxiong Deng, Shicheng Wang, Wanlu Hong: Institute of Ultrasonic Technology, Shenzhen Polytechnic University, Shenzhen, 518055, China

titanium alloy is a light but not super strong element when the weight of low carbon steel is about 45%. Titanium alloy is usually mixed with other metals to make it super stronger. The metallurgists had tried to mix titanium with free iron and also together with vanadium and aluminum 50 years ago [48,49]. Similarly, magnesium is the eighth most abundant metallic element in this universe. It is well known that magnesium is either extracted from the ocean or obtained from minerals such as in the form of dolomite or magnetite [35,50–52]. It is further considered lighter than titanium and aluminum. This is due to its unique physical properties, shape, and high cost [53,54]. It is used in the high-end frame market for interior designers of many buildings [55]. Likewise, titanium is considered much lighter than copper metal. In the market, titanium is much more expensive than copper metal. However, copper metal is a better conductor of heat than titanium [56–58].

The industrial sector is looking for the cheapest and most cost-effective method of joining similar and dissimilar metals. So, the ultrasonic welding process is a well-known and straightforward method for joining different materials to provide an effective and advantageous way for various industries such as aerospace and automotive [59–62]. This review article reports a detailed literature study regarding metallic alloys and their welding performance based on the ultrasonic welding process. It is stated that the advantages of using ultrasonic welding over conventional joining methods for automotive applications such as the car industry are also thoughtful and cost-effective. The important characteristics and physical parameters of ultrasonic equipment considered useful for ultrasonic welding machines are discussed in detail in this review study. Moreover, the different process parameters for different metal alloys explained the weld quality, fatigue, and cracking behaviors of the materials. We present a detailed survey covering ultrasonic metal-to-metal welding and also provide some literature on metals to other materials. New efforts to join dissimilar metals are presented, which may be of considerable interest to a scientific and industrial community to refer to for new ideas in the future. The recommendation for future research directions based on the research gap in the field of ultrasonic welding technology is also discussed in the last part of the article.

1.1 Joining techniques for lightweight alloys

The lightweight metals are used to manufacture high-strength composite parts such as forming aircraft wings, motor vehicles, or motor car bodies that require a large and complex mould. Since, this means a significant increase in the cost of automobiles. However, such a complex part can be produced through the assembly of small parts using various joining techniques. There are several joining techniques used to join similar and dissimilar lightweight metal materials as shown in Figure 1. For aluminum alloys, the strength of the clinching joint is probably 2,000 N which exposes its weak behavior [63]. The strength of the clinching joint has many economic advantages compared to SPR because it does not use rivets. This is a cost-effective method. However, the disadvantage of the clinching joint is that it has low strength and cannot be applied in many industrial processes [64–66]. The results in the literature state that the strength increase is more than 200% compared to the SPR process but still not enough. So it shows that the welding results are not useful for the manufacturing industry. The bar extrusion needs high initial cost or setup for joining two similar or dissimilar metals. Likewise, high compressive force is required to initiate the process [67]. So, it is not easy to implement bar extrusion at the commercial level. The cost of hot and cold forging for heat treatment is very high and they have a less precise dimensional tolerance including the risk of distortion and residual stresses [32,67,68]. The main disadvantage of friction stir welding is the creation of holes or voids when welding similar or dissimilar specimens. At the joints of the spikes, holes are created to make the specimens weaker in the specific position. The stress concentration also increases due to the positions of the voids in the riveting joints. Likewise, hydroforming is capable of producing complex joint shapes in the industrial sector but must exert high pressure which makes industrial products very expensive [64].

The conventional methods used in the industry for assembling a large number of light metals are mechanical fastening using rivets and bolts, joint co-consolidation, and chemicals [69–72]. Lightweight metals joining methods namely riveting and rolling, gluing, friction stir welding, and ultrasonic welding are the most common joining techniques in the industry [73,74]. Ultrasonic welding has emerged in recent years as a new type of solid-phase welding technology which is suitable for high-strength joints of light alloy sheet materials [75]. Similarly, the ultrasonic welding method is more efficient for joining metals compared to conventional methods [76]. The benefits of using the ultrasonic welding process are that it has a wide range of applications in the automotive industry. It can be applied to the welding of a variety of combined materials and can further perform rapid spot welding and continuous welding [77]. The ultrasonic welding has incomparable advantages in welding the similar and dissimilar metals compared to mechanical fastening methods.

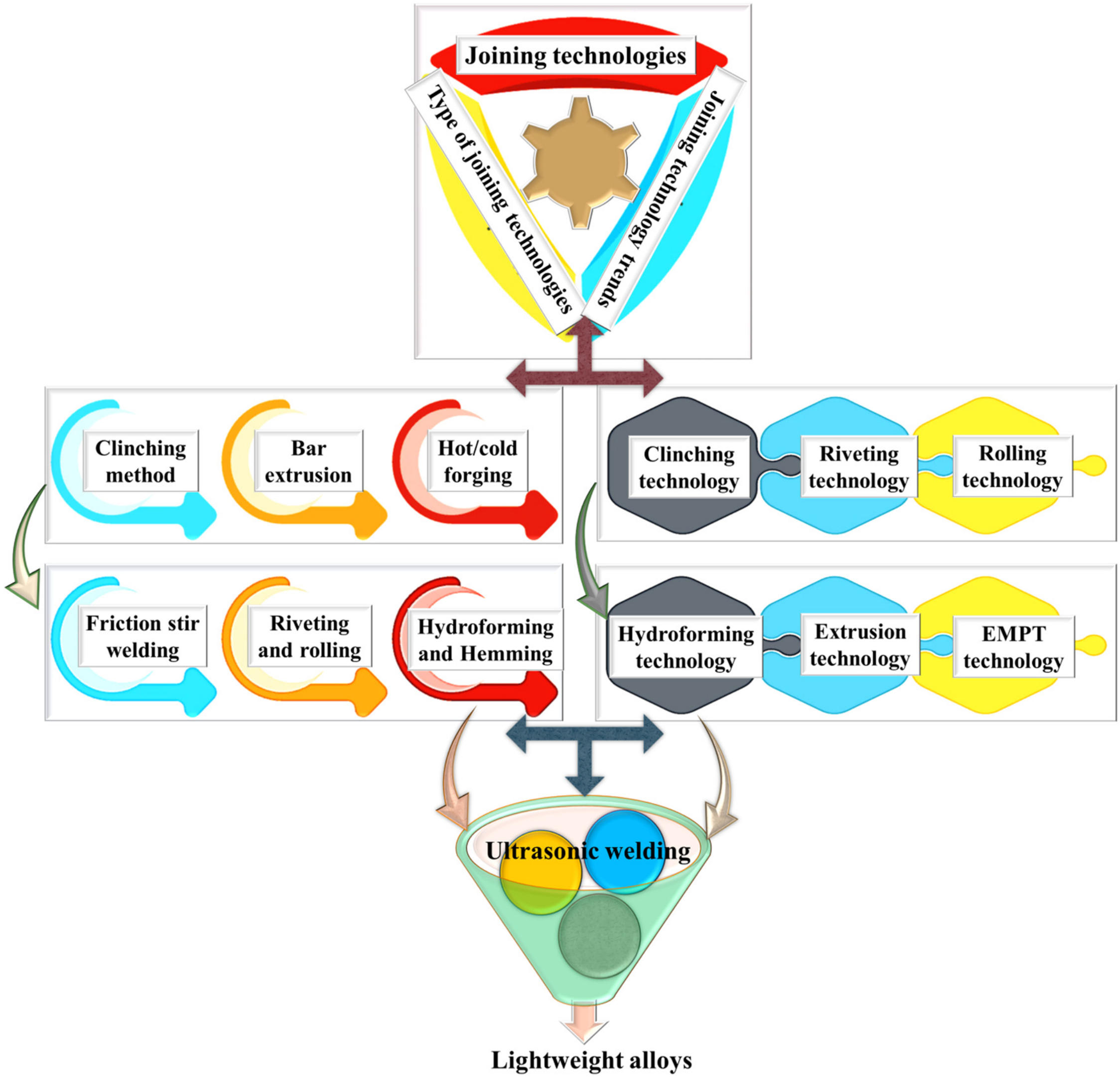

Figure 1: The comparison of different joining techniques for welding similar and dissimilar specimens [36].

Ultrasonic welding itself can clean oxide films from the surface of the workpiece. So the surface cleanliness of the workpiece is not high and a small amount of oxide film and oil stains are allowed [78,79]. Moreover, only high local temperature is generated during welding and there is no need to cool the weld. The welding deformation is small and the welding process does not require the participation of flux and external sources of heat. There are no welding slag and gas residue during the operation [80]. In addition to the above-mentioned pros of ultrasonic welding, there are still some challenges in the design, process manufacturing, and quality inspection of the acoustic system [81]. Figure 2 illustrates the different perspectives of this review study. The narrative regarding the wide range of application, advantages, and some of the main challenges is discussed in the flow diagram. At present, ultrasonic metal welding mainly includes four series: ultrasonic metal spot welding, wire harness welding, metal sealing and cutting, and metal roll welding [82–85]. It is widely used in automotive interior parts, electronics, electrical appliances, motors, refrigeration equipment, hardware products, batteries, solar energy, transportation equipment, toys, and other industries [51,54,86,87].

This review article summarizes the research progress of ultrasonic welding of aluminum alloy, magnesium alloy, and titanium alloy homogeneous and dissimilar thin plates in recent years. The characteristics of each alloy and the principles and equipment configuration of ultrasonic welding are also briefly summarized. Furthermore, the study will outline the process parameters of ultrasonic metal welding and look forward to the future development direction.

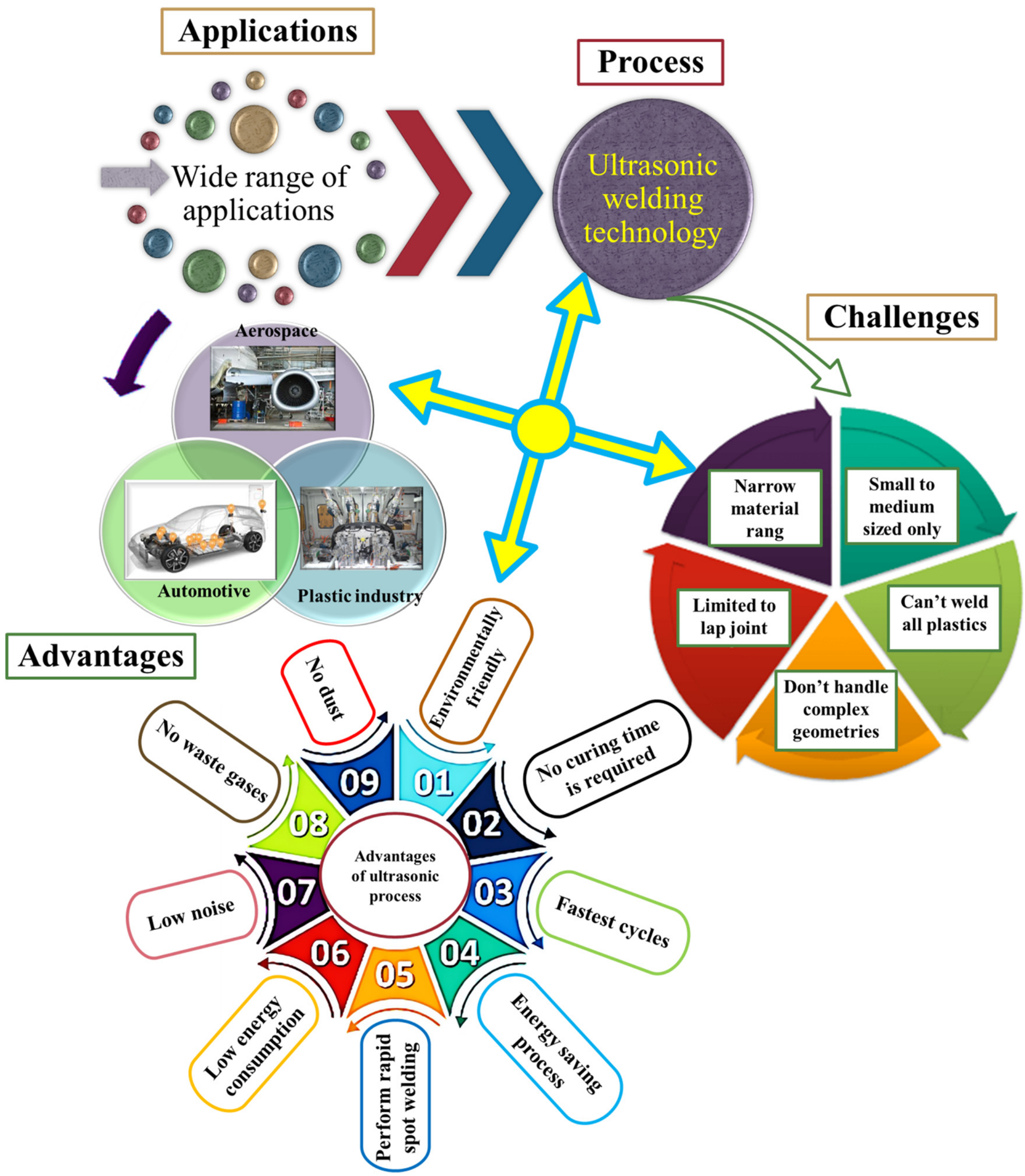

Figure 2: The detailed flow chart for applications, advantages, and challenges of the ultrasonic welding technique [16,38].

2 Ultrasonic welding process

2.1 Working principle

The oxide film from the surface of the material is removed by applying ultrasonic vibration in the ultrasonic metal welding process. The impurities from the surface layer are dispersed and the attractive force between metal atoms is used to create a solid phase bonding state [88]. The schematic for the principle of ultrasonic metal welding is shown in Figure 3. The ultrasonic generator converts the 50 Hz power frequency current into a high-frequency current of 15–80 kHz. The high-frequency current flows through the transducer coil to generate a high-frequency alternating magnetic field [89–91]. The ferromagnetic material is alternately stretched longitudinally due to magnetostriction which is converted into elastic mechanical energy. Then, it is amplified by the horn, and finally, the elastic vibration energy is transferred from the upper sound level to the workpiece [92]. The vibration direction of the welding head is parallel to the surface of the weldment when the workpiece material is metal. Likewise, its vibration energy is transmitted to the surface of the workpiece along the tangential direction [93]. So, it causes the relative friction between the welding head, the workpiece, and the base of the system as shown in Figure 3. The dynamic friction between the weldments removes the oxide film and pollutants on the surface of the workpiece [94,95]. Under the action of welding pressure, the surface of the pure workpiece fits tightly. At the same time, it is accompanied by the plastic deformation of the workpiece. The plastic flow of the interface and the metallurgical reaction for the dynamic recrystallization eventually achieves a solid-state weld [96,97].

2.2 Ultrasonic welding equipment

Ultrasonic generator: The ultrasonic generator is a key device in ultrasonic welding and provides high-frequency waves. It is used to generate electrical energy which is further used by the transducer and converted into mechanical energy [98].

Transducer: A transducer is an electronic device that converts energy from one form to another. Different types of transducers are used in different fields and common examples include microphones, loudspeakers, thermometers, pressure sensors, and antennas [99].

Horn/sonotrode: The horn or sonotrode is a key part of the ultrasonic device [100,101]. The horn is attached directly to the specimen. The electrical energy is converted into mechanical energy and then transferred directly to the sample with the help of the horn. Basically, the horn produces friction which transfers the mechanical vibrations to the metals which will then be welded.

Luffing lever: A device is used to apply load and thrust the horn and produce high impact for the mechanical energy coming from the transducer. The luffing lever is used as an amplification device between the transducer and the horn [102].

Upper and lower sound level: The upper and lower parts are used to fix and adjust the specimens in the

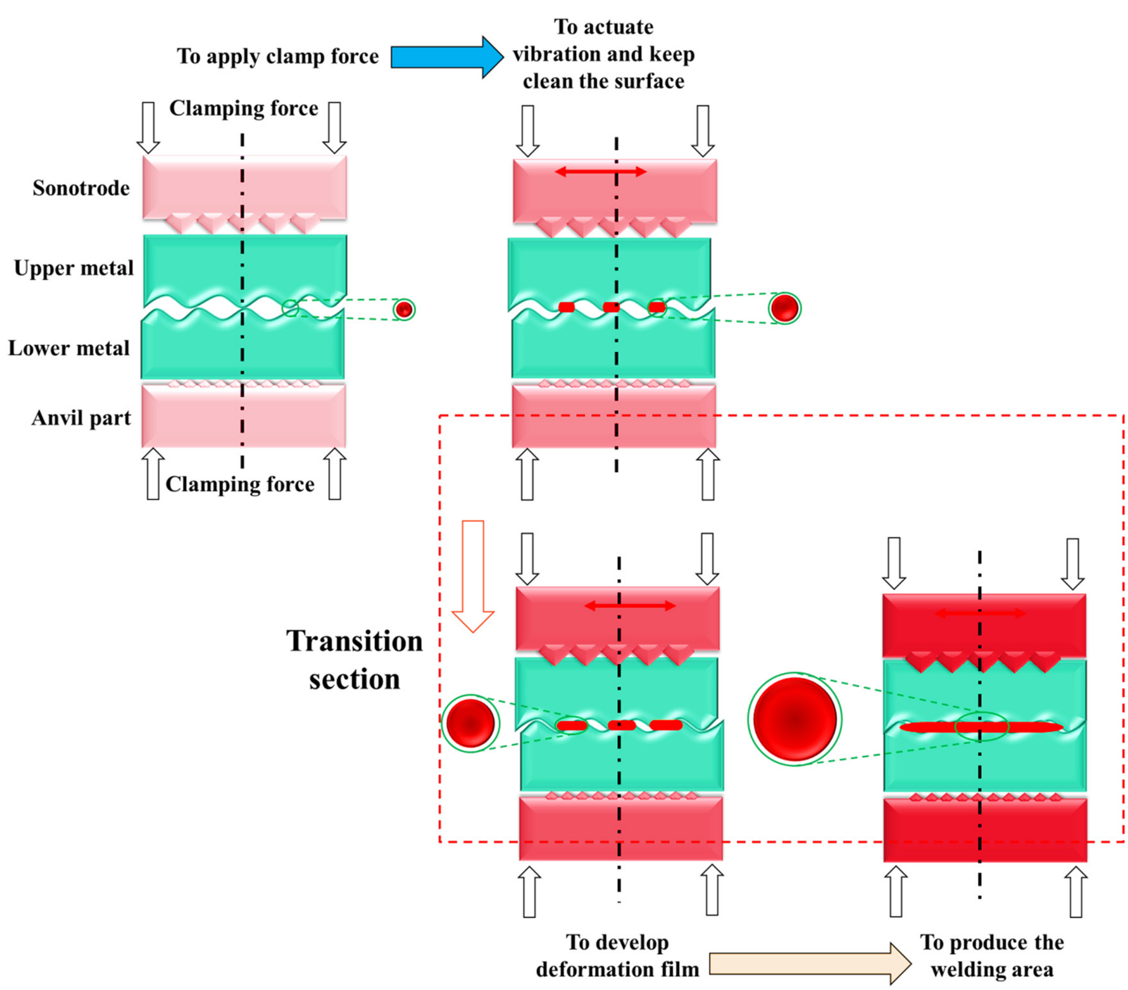

Figure 3: The working principle of ultrasonic welding process [42].

ultrasonic welding process. The parts work as intermediary units for the welding process to tighten the metal materials [103].

Workpiece/specimens: The workpiece or specimens are used to create a weld joint on a particular surface. The workpiece is a distinctive material which can be a metal or a plastic during ultrasonic welding. The workpiece can be used in different shapes or patterns to adjust the welding process and avoid fracture, fatigue, and high-temperature effects. Figure 4a and b illustrates the schematic diagram and experimental setup of the ultrasonic welding equipment which elaborates the whole joining process for similar and dissimilar metals [104,105].

2.3 Types of ultrasonic welding and process parameters

The ultrasonic welding is used to join similar and dissimilar metal combinations and plastic materials. It is familiar and useful for metals to metals, thermoplastics to thermoplastics, and the same for dissimilar materials such as metals with thermoplastics to be joined for different application sectors [106]. Principally, ultrasonic welding is categorized into two types: ultrasonic plastic welding and ultrasonic metal welding. The welding of metals during the ultrasonic process is different from the welding of plastics in terms of the working principle. The vibration of the welding head in metal welding

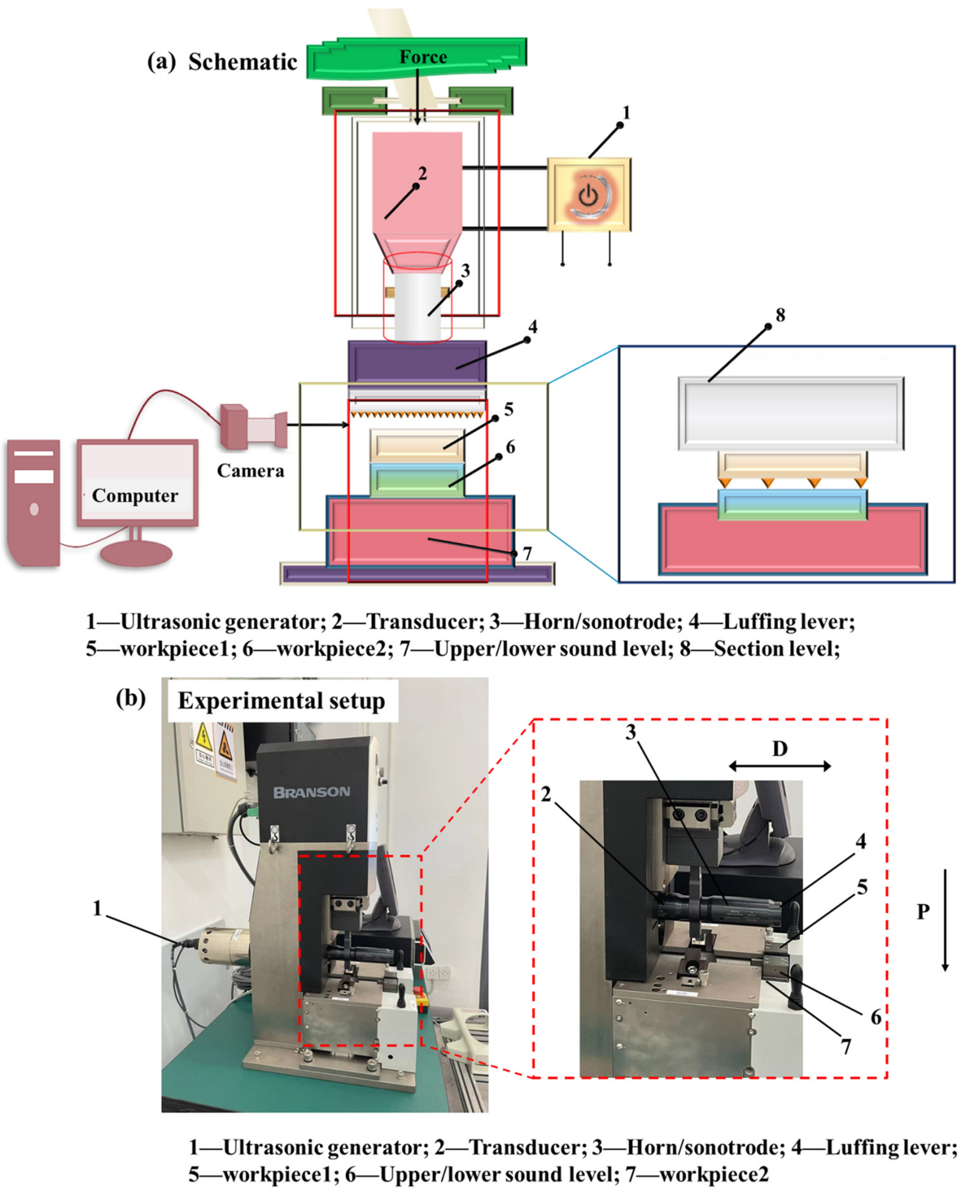

Figure 4: The construction of ultrasonic welding equipment: (a) schematic diagram and (b) experimental setup photograph.

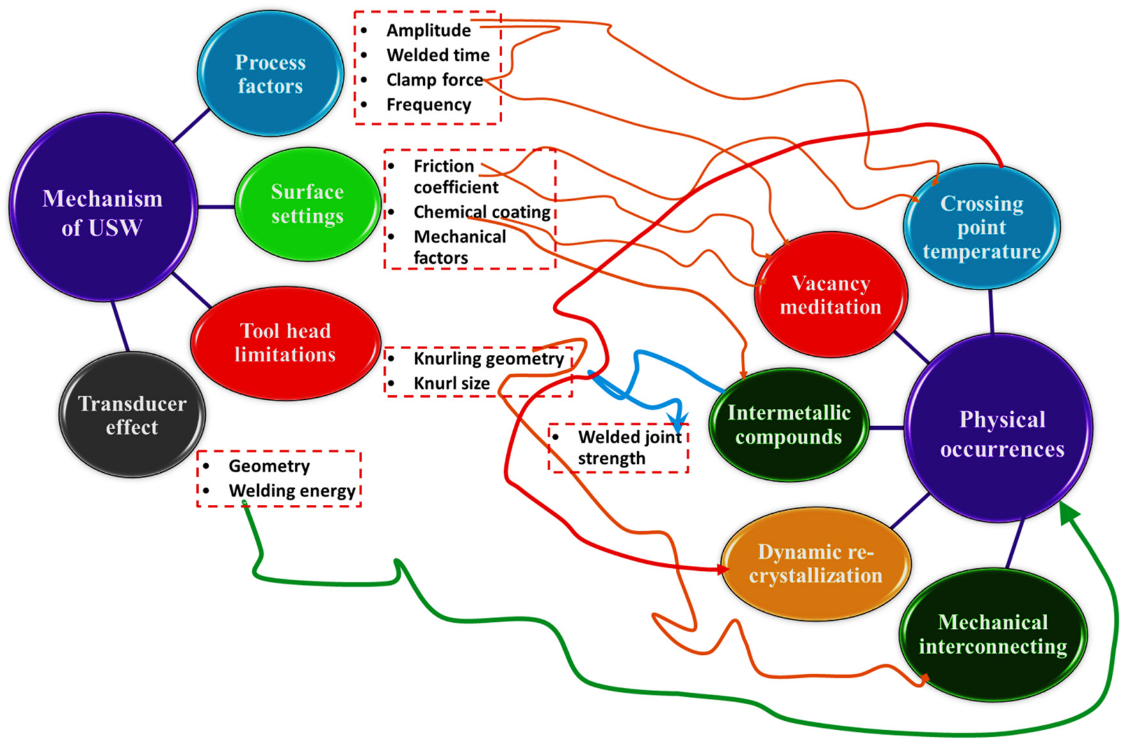

Figure 5: Steps for ultrasonic welding mechanism along with operational parameters of material and tool head [15].

is parallel. However, the head moves in the perpendicular direction where the weld is focused on the plastic weld. Figure 5 shows steps for ultrasonic welding mechanism along with operational parameters of material and tool head.

Figure 6 explains the details of the types of ultrasonic welding process. Figure 6(a) illustrates the schematic of ultrasonic welding of plastics and metals. Likewise, Figure 6(b) shows the flow diagram of changes in ultrasonic plastic and metal welding [107–109].

The mechanical properties and macrostructure and microstructure changes in ultrasonic-welded joints mainly depend on the adopted process parameters including ultrasonic frequency, amplitude, clamping force, power, and energy.

2.3.1 Frequency

The centre frequency for ultrasonic welding machines is applied with a range of 20–40 kHz and its working frequency is mainly determined by the mechanical resonance frequency of the ultrasonic transducer, horn, and welding head. The frequency of the ultrasonic generator is adjusted according to the mechanical resonance frequency to achieve high stability and consistency. So the welding head works in resonant mode and each part is designed as a half-wavelength resonator during the process. The sonotrode and the mechanical resonance frequency together have a working resonance range in the whole working condition. It is generally set to ±0.5 kHz and the welding machine can basically operate normally within this range. We adjust the resonant frequency when the welding head is produced and the error between the resonant frequency and the design frequency is required to be less than 0.1 kHz [110,111].

2.3.2 Amplitude

Amplitude is a key parameter affecting joint quality which can transfer mechanical energy to the welding interface [112]. The amplitude is typically in the range of 10–100 µm. The amplitude is a dependent variable in some welding machines. It is related to the welding time or the energy applied to the welding machine. In other machines, vibration amplitude is an independent variable. Thus, the impedance is set and adjusted by supplying power due to the added characteristics of a feedback control system. The selection of the welding vibration amplitude depends on the welding conditions determined by the material [113].

2.3.3 Clamping force

The clamping force is an important parameter in the ultrasonic welding process and its selection depends on the

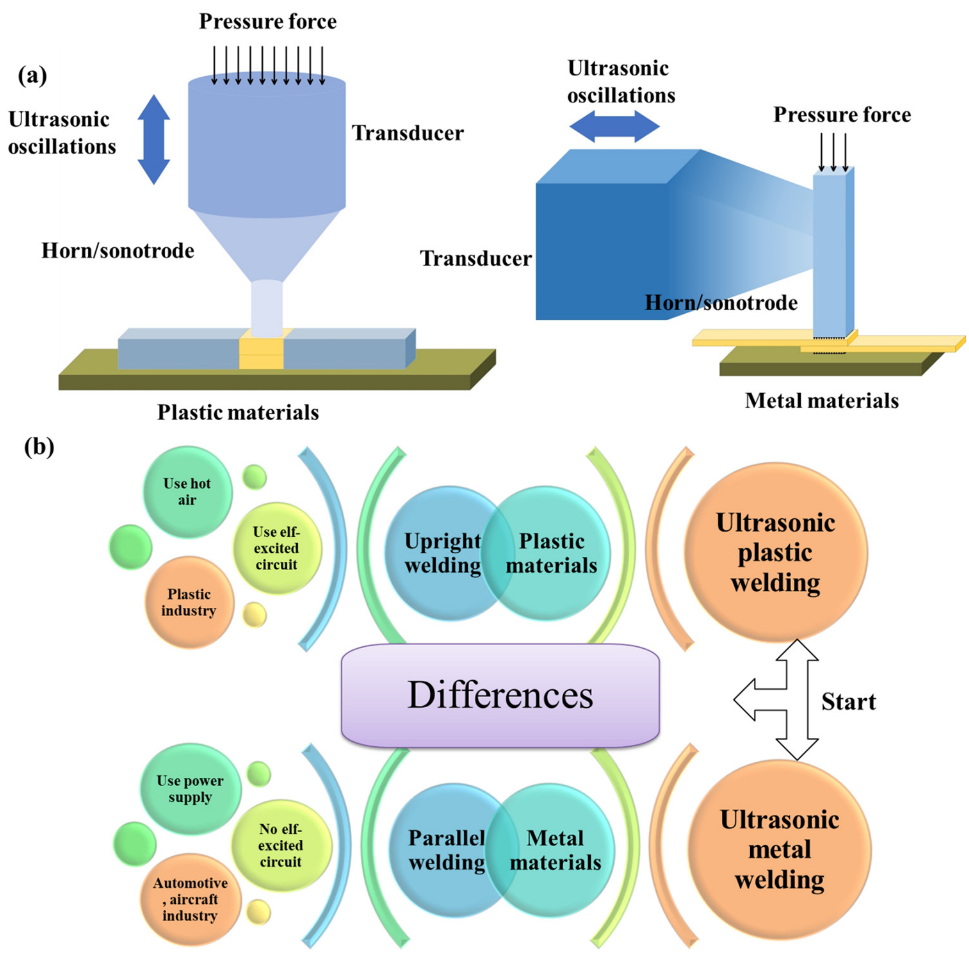

Figure 6: Types of ultrasonic welding process: (a) schematic of ultrasonic plastic and metal welding and (b) flowchart of differences in ultrasonic plastic and metal welding [40].

material being welded. So, the optimal clamping force can be achieved by adjusting welding parameters below which the joint will be weak to non-existent. Therefore, if this parameter is exceeding the thinning of a weld zone, then sticking of the sonotrode will occur [114].

2.3.4 Power and energy

The ultrasonic welders can be set to operate in either time or energy-controlled modes. So, the energy and time can be interchanged. Figure 7 explains the complex relationship between peak power and welding energy to the transducer. The area under the power curve is the welding energy. It can be seen that power, energy, and time are not independent. Once the power is set and the welding process proceeds, then a certain power level can be reached to develop transition in the process [46]. The welding energy and time will also reach specific values under the specific power values. Similarly, the setting time will continue the welding process until a certain energy level is attained. In practice, the time for energized curve can take various forms depending on the material type, size, surface condition, amplitude, clamping force, tool, and specific characteristics of the stationary welding machine

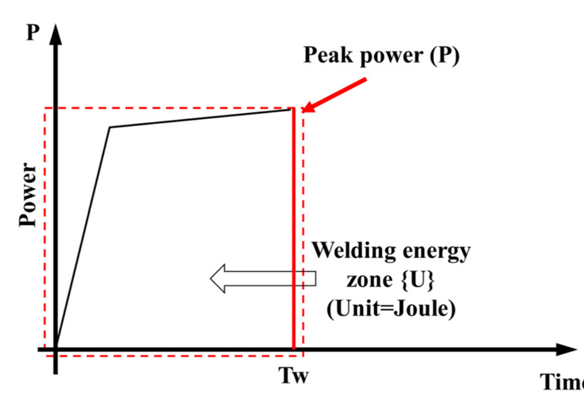

Figure 7: The relation between peak powers, welding energy, and time duration.

[115]. Figure 7 illustrates the relationship between peak powers, welding energy, and time duration curve.

3 Research progress of ultrasonic welding for lightweight alloys

3.1 Research progress of aluminum alloy in ultrasonic welding

He et al. introduced the vacuum diffusion welding process to test the microstructure and properties of Cu/Al diffusion welding joints. The research showed that an obvious diffusion transition zone was formed at the interface during Cu/Al diffusion welding. Moreover, the microscopic interface is appeared. The hardness peak value was measured to HV780. According to the analysis, intermetallic compounds are generated in the transition region on the copper side. The generation of intermetallic compounds at the interface can be avoided or reduced by controlling the diffusion concentration of Al [116]. Milewski et al. established a three-dimensional ultrasonic welding heat-structure coupling ANSYS finite element model. The study simulated the ultrasonic metal welding process of 6061 aluminum alloy. The results showed that the error between the simulation value and the test value of the maximum temperature in the welding area is within 5%. The highest temperature is located in the centre of the welding area and the high-temperature area increases with the increase of welding time during the ultrasonic metal welding process. The temperature field is mainly affected by welding pressure and welding time [117]. Lee et al. studied the microstructure of ultrasonic welded joints between 6111-T4 aluminum alloy and galvanized high-strength low-alloy steel. The studies have revealed that the rapid interdiffusion of Zn and Al during welding due to rapid heating and high strain rates leads to the formation of an Al–Zn eutectoid/eutectic interface layer [118]. At higher welding energies, a portion of this diffusion layer is pushed out of the nugget edge which created an additional brazing effect. Haddadi et al. studied the grain structure, texture, and mechanical property evolution of 6111-T4 aluminum plate during high-power ultrasonic welding. The study has determined that a large amount of deformation is induced in the weld zone where the temperature rises to 440°C. Thus, an ultrafine-grained structure was observed in thin ribbons on the flat welding interface during the short welding time of 0.1 s. As welding time increases, the interface displaces, and “wrinkles” or “peaks” and shear bands appear. The welding interface gradually changes from flat to sinusoidal when it fully penetrates the workpiece. Finally, a spiral waveform with a wavelength of about 1 mm is generated after 0.4 s [119–121]. Ni et al. studied the effect of interlayer of 2219 aluminum particles on the performance of ultrasonic welding of Al–Ni dissimilar materials. It determined that the interlayer is beneficial to increase the temperature of the welding interface and improve the solderability. Thus, it successfully gained a good Al–Ni connection. Simultaneously, an interfacial diffusion layer was generated in the welded interface and a large number of welded areas were observed on the fractured surface. So, the interlayers increase the maximum tensile shear load while reducing the welding time [122].

Shin et al. studied the ultrasonic spot welding parameters of the A5052-H32 alloy plate. The mixed shear and tensile failure mode exhibits higher lap shear failure loads while separate shear and pull is the prominent failure mode at lower lap shear failure loads. Therefore, shorter welding times are required with higher vibration amplitudes to generate sufficient temperature and prevent excessive adhesion [123]. Peng et al. presented the microstructure and mechanical properties of ultrasonic spot welding of aluminum alloy 6022-T43. The effect of welding energy is determined. It was found that due to the occurrence of dynamic crystallization, an ultra-thin necklace-like equiaxed grain structure (having approximately equal dimensions in all directions, especially of a crystal grain in a metal) was observed along the weld line. Smaller grain sizes at lower welding energy levels are obtained. Tensile lap shear strength, failure energy, and critical joint stress intensity were initially increased. Then, the decrease with increasing welding energy reached a maximum level [124]. Mirza et al. studied the microstructure and fatigue properties of ultrasonically spot welded joints of aluminum alloy 5754. Tensile fracture occurs at the Al/Al interface at lower energy inputs and at the edge of the nugget zone at higher energy inputs. The maximum cyclic stress at which the fatigue fracture mode switches from transverse crack propagation through the thickness to interface failure increases with increasing energy input [125]. Hoehr et al. proposed a method for evaluating the shear strength distribution in the lap area of ultrasonically welded single lap joints of aluminum and fiber-reinforced thermoplastics. The force is not distributed uniformly in the connection area and consists of connected and cohesive parts under study. For evaluation, two procedures were developed to divide the bonding area into parts and study them separately. So, subsequent mathematical operations have determined the local intensity distribution in the junction region, which allowed the identification and assignment of different binding mechanisms [12]. Dhara and Das analyzed the macroscopic and microscopic structures of various Al–Cu joint welds. The research showed that mixing

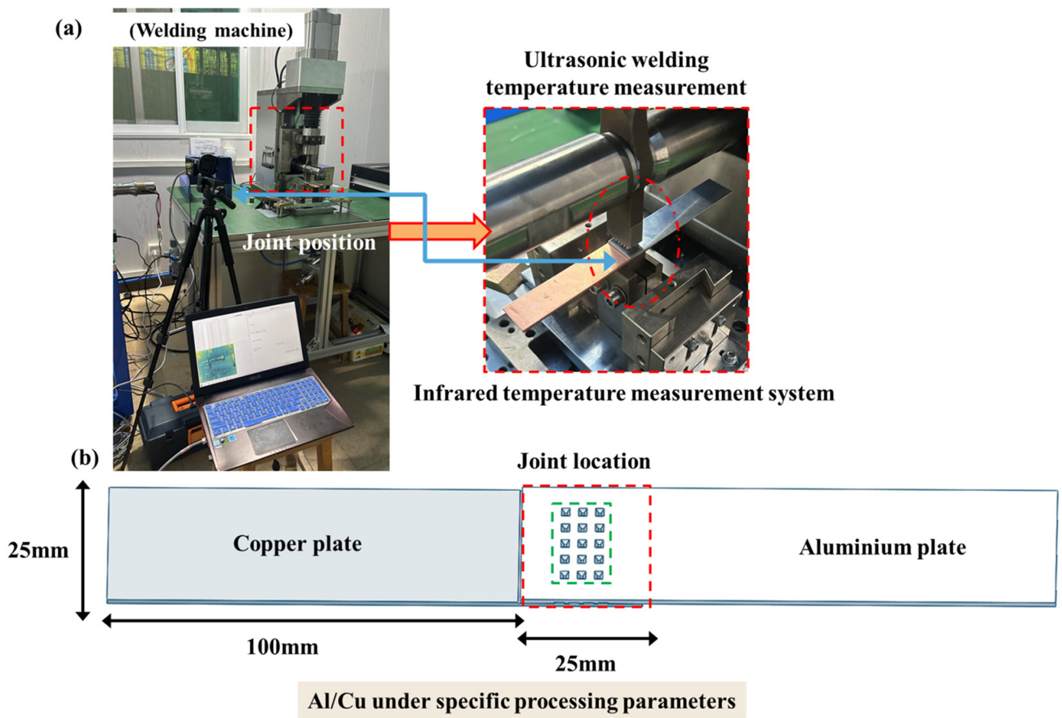

Figure 8: The (a) real experimental photograph and (b) schematic diagram of the infrared temperature measurement system in ultrasonic welding process. Reproduced with permission from MDPI publisher [15].

of material at the interface, wavy material flow, and the formation of interface micro-bonds are the main reasons for the better effect of ultrasonic welding [126]. Liu et al. systematically studied the bonding mechanism of Cu–Al high-power ultrasonic welding interface and the formation mechanism of interfacial metal compounds. It was investigated that the grain size of pure copper along the welding interface does not change much under the action of welding pressure and ultrasonic vibration. However, aluminum alloy microstructures are transformed from elongated grain sizes to equidistant grain spacing (the structures have the properties that each atom is intermediate from each of its nearest neighbors). The grain structures with equal grains are obtained by exploiting great technological and functional properties when the time varies from 0.3 to 0.5 s. The time interval increases rapidly and the grain size transforms from 1.54 to 5.89 µm. The aluminum alloy forms a Gaussian {110} texture and a rotational cubic {001} texture along the weld interface [127]. The crystal lattice defect of copper diffuses significantly faster through the aluminum matrix at the weld interface. It results in the closure of copper atoms and the excess of aluminum atoms which is the reason for the formation of the single metal compound $CuAl_2$ in the ultrasonic welding process [47]. Figure 8a illustrates the real experimental photograph. The schematic diagram of the infrared temperature measurement system in the ultrasonic welding process is shown in Figure 8b. Figure 9 shows the relation between copper and aluminum cross-sections under optimized parameters (e.g., (a) associated with Al cross-sections (b) associated with Al cross-sections under different locations and (c) associated with Al and Cu cross-sections).

3.2 Research progress of magnesium alloy in ultrasonic welding

Jasmin et al. studied the fatigue life evaluation of ultrasonic magnesium alloy AZ31B-H24 using spot-welded joints. The study estimated that ultrasonic welding has a longer fatigue life compared to other welding processes. The fatigue damage mode varies from interface damage to transverse crack expansion along the thickness direction with reduced levels of cyclic loading depending on the weld energy. A life prediction model for spot-welded lap joints was developed by Newman and Dowling to estimate the fatigue life of ultrasonic magnesium alloy joints [129]. Macwan and Chen used ultrasonic spot welding to join rare earth containing ZEK100 Mg alloy at different welding energy levels. The study noted that dynamic recrystallization occurs in the molten core region. The grain size increases with increasing interface temperature and strain rate under study. Microhardness was decreased and welding energy increased throughout the testing process. Similarly, the relationship between grain size and Zener–Hollomon parameters was established [130]. Additionally, the Petch-type relationship between microhardness and grain size was established by Arghavani et al. [131]. Meanwhile, Macwan et al. investigated the feasibility of ultrasonic spot welding of heterogeneous joints ZEK100–A15754 and evaluated the interface microstructure, tensile lap shear strength, and fatigue life. The study states that the tensile and shear strength of the joint increases initially and reaches a peak and then decreases with increasing welding energy. The best average joint strength is close to 78% of the same joints for ZEK100–ZEK100 and 55% of the same joints for A15754–A15754. The bilinear behavior of the S–N curve fits well with the variation of damage characteristics. Thus, the interfacial damage dominated while at lower cyclic load levels through-thickness cracks formed at the edge of the melt core [30].

Čiripová et al. evaluated the microstructure formation mechanism and weldability of long periodically ordered structural phase Mg–Zn–Y alloy. For the first time applied the ultrasonic spot welding technique in welding. It was found that the microstructural evolution of the joint depends on the macroscopic shape of the weld nozzle in the flat and inclined areas. A fine-grained band is created around the weld interface. In the slope zone, new wave bands are generated and reveal that plastic flow occurs in all bands. Likewise, Zn and Y deviate at the grain boundaries of the Mg matrix out of band in the flat zone. Moreover, the maximum weld strength was obtained under the welding conditions that produced a new strip. It was found that increased plastic flow in the sloped zone contributed to increased weld strength [132]. Ji et al. performed ultrasonic friction stir welding (UaFSW) to improve the quality of Al–Mg joints. It was shown that the ELW of Al–Mg FSLW alloy joints were enhanced by the addition of Zn foil and external ultrasonic

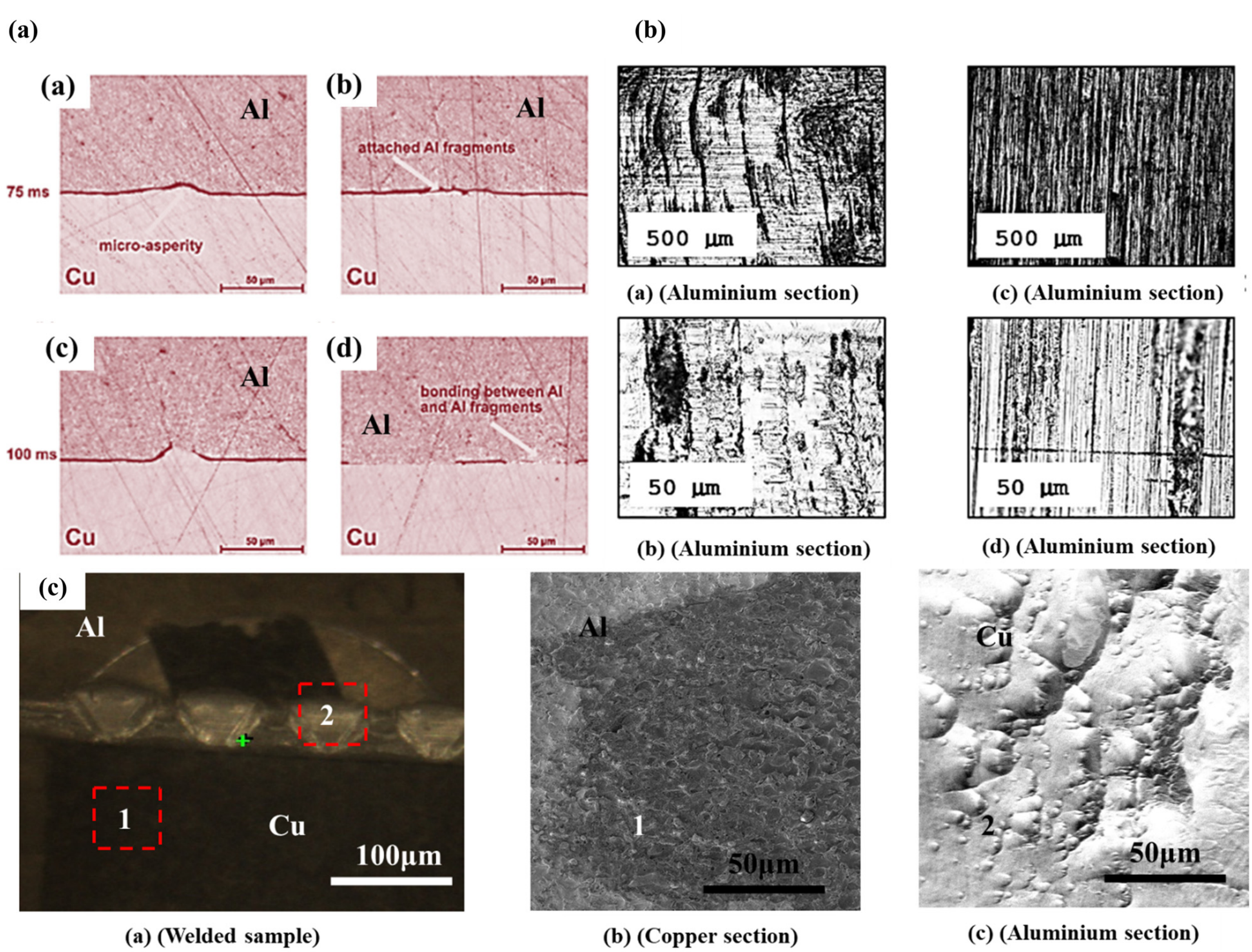

Figure 9: The relation between copper and aluminum cross-sections under optimized parameters (a) associated with Al cross-sections (b) associated with Al cross-sections under different locations and (c) associated with Al and Cu cross-sections. Reproduced with permission from IOP-MDPI publisher [39,128].

assistance. Discontinuous Mg–Zn IMCs replace continuous Al–Mg IMCs due to the addition of Zn foil. Furthermore, the Mg–Zn IMCs are uniformly distributed in the SZ due to the external ultrasonic assistance which effectively improves the tensile shear load of the joint. The load increases with increasing ultrasonic power and the maximum tensile shear load reaches 7.95 kN which is 52.6% greater than that of conventional joints. Likewise, the hybrid process of Zn foil and external ultrasonic assistance has significant advantages for improving the quality of Al–Mg FSLW alloy joints. It promotes ultrasonic power within a reasonable range and may further improve joint quality [133]. Wang et al. performed the ultrasonic welding process to improve the quality of various alloy (Al/Mg) joints. The effects of laser texturing on the microstructure and mechanism of the ultrasonically welded AZ31B/5052 joint were also investigated. The quality of the formation of welded joints was improved [134]. In the Vickers hardness test, the weld hardness distribution pattern was taken as dispersion diffusion from the central region. The hardness in the central region was the highest during the test. The microscopic morphology of the weld head under different pressures from the increase in welding pressure and the microscopic morphology of the weld interface have different phase characteristics. Since, weak bonding phase (0.2, 0.3 MPa), corrugated phase (0.4 MPa) and folding phase (0.5 MPa) are discussed by researchers. Therefore, corrugated phase (0.4 MPa) has the most reliable mechanical properties and the best welding results [135,136]. Figure 10a and b shows the fracture analysis of cross-sections in low energy Mg–Al-welded joints. Figure 10c demonstrates the groove surfaces in cross-sections of Mg welded joints with low applied energy

3.3 Research progress of titanium alloy in ultrasonic welding

Dewang et al. studied the effect of welding parameters on tensile and fatigue properties of ultrasonically welded magnesium–titanium heterogeneous joints. The study

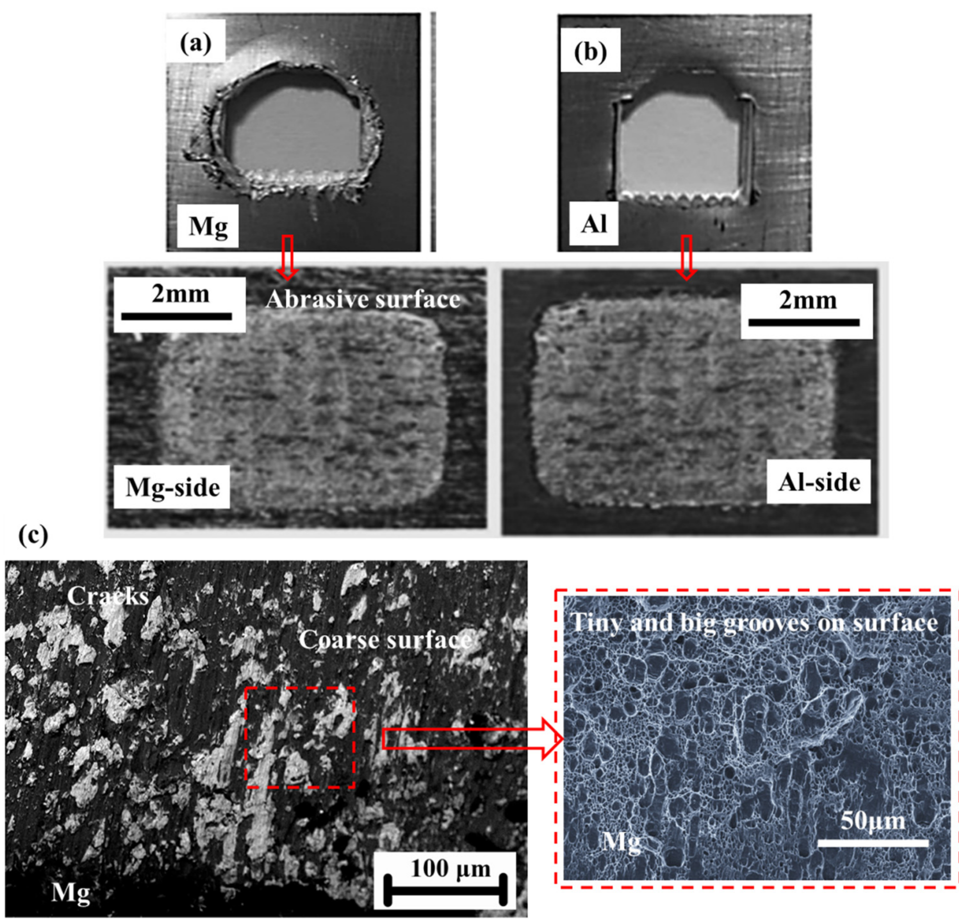

Figure 10: The fracture analysis of cross-sections in Mg–Al-welded joints at low energy: (a) fractures in Mg cross-section, (b) fractures in Al cross-section, and (c) grooves surfaces. Reproduced with permission from Elsevier publisher [137].

pointed out that tensile property and welding pressure is the most important influencing factor. Welding time and welding amplitude are also considered very important parameters for joining metals. Furthermore, the interaction between welding time and welding amplitude has a significant effect on performance. The failure mode of the joint is different at different numbers of cycles when the joint reaches high bond strength. Thus, the thickness of the magnesium plate will lead to a reduction side while applying very high welding parameters. It will significantly reduce the fatigue performance of welded parts where the influence of welding pressure is most important [138,139]. Aubert and Duval studied through interactive orthogonal test design that tensile load and joint signal-to-noise ratio as an evaluation index for process optimization of aluminum/titanium dissimilar metal ultrasonic welding parameters are favorable for metals. The results showed that the welding parameters in the main order energy > amplitude > pressure follow the contribution of tensile load 86, 8, and 4%, respectively. The process parameters are used to obtain the maximum tensile load for the combination of energy 950 J, amplitude 75 mm, and pressure 0.552 MPa (A3B2C2). These are also used to obtain the most stable tensile load for the combination of energy 900 J, amplitude 70 mm and pressure 0.621 MPa (A1B1C3) [140]. Zhu et al. analyzed the cross-sectional morphology and its mechanical properties of Ti6Al4V titanium alloy joints under different ultrasonic welding process parameters through scanning electron microscope observation and tear tests. The results showed that the reduction rate in the cross-section of the joint increases with the increase in the welding time which is a decisive factor in the quality of the welded parts. The optimal welding time for Ti6Al4V titanium alloy with a static pressure of 1144.53 N is 125 ms which has the highest interfacial bond strength [141]. Zhou et al. studied the effect of welding time on the organization and mechanical properties of ultrasonic spot welding of AA6061 aluminum alloy and pure titanium thin plates. The study revealed that no intermetallic compounds were found at the joint interface. Thus, the maximum joint loads increase with the expansion of the joint area with the increase of the welding time under study [142]. Then, it decreases due to fatigue cracking on the Al side. The peak temperature increases with increasing welding time. In the weld zone, the aluminum alloy softened through the welding energy while the hardness of pure titanium did not change significantly [143–145]. Zhang et al. studied the interfacial segregation of alloying elements during ultrasonic heterogeneous welding of aluminum 6111 and titanium Ti6Al4V. The study noted that enrichment of silicon, magnesium, and oxygen was found at the Al/Ti interface. However, other alloying elements such as copper and vanadium were not completely separated. Thus, 4% of Si was found at the Al/Ti interface within a very short welding time of 1.4 s. The distribution of unidirectional Si is inversely proportional to the distribution of O and Mg [146]. So, the residual oxides and segregated of Si at the Al/Ti interface can be an obstacle to the nucleation and growth of Al3Ti. The strong chemical attraction between Ti and Si may be the driving force behind the tilting of Si toward the Al/Ti interface. The presence of discontinuous oxides at the Al/Ti weld interface can reduce the mechanical properties of the weld [147–149]. Ma et al. used UaFSW to join aluminum 6061-T6 and titanium alloy Ti6Al4V (TC4). It was found that ultrasonic waves improved the diffusion thickness and reduced the average grain size. The titanium alloy fragments and the bottom interface of the UaFSW joints formed a hook-like structure that improved the bond length and mechanical interlocking [150]. The microhardness of the stirring zone increases due to further refinement of the grains by ultrasound. The maximum tensile strength of UaFSW joints was 236 MPa, reaching 85% of 6061-T6-based joint and 54 MPa higher than that of conventional joints [151–154]. Boumerzoug and Helal investigated the friction stir welding of dissimilar materials such as aluminum (AL6061-T6) to ultra-low carbon steel. The tool head of the fixed ultrasonic device was placed on the back of the workpiece to apply ultrasonic vibration for welding materials. Figure 11a and b indicates the lap joints of aluminum alloy 6061-T6 and titanium alloy TC4 that were welded under ultrasound-assisted conditions by applying ultrasound to the aluminum and titanium plates, respectively. It was found that when ultrasound was applied to the aluminum side, the pinhole defects appeared at the hook of the aluminum/titanium interface. The hook height at the interface is higher compared to the application of the ultrasonic tool head on the titanium side [155]. Furthermore, the hook holes defect will become a crack source and generates stress concentration. Therefore, the joint is subjected to a greater load. The results explained that the effect of ultrasonic vibration applied on the side of the titanium plate is better than that applied on the side of the aluminum plate [156]. Figure 11 illustrates the schematic diagrams of the Xenophilic and Xeno Al/Ti structure applied ultrasonically to the bottom surface of the titanium alloy.

Lin et al. studied the interfacial phenomena during ultrasonic welding of ultra-low carbon steel with pure titanium. It was found that when the temperature of the joint was increased above 600°C during USW, the bonding strength increased drastically and resulted in base-metal fracture. Thus, the analysis of interfacial scheme, fracture, compositional phase and crystallographic indicated that the phase transition of Ti from α (hexagonal close-packed) to β (body-centered cubic) leads to the improvement of high-temperature deformability. It further facilitated the elimination of voids near the bonding interface [157]. Wang et al. investigated the interplay of microstructures and mechanical properties of WC-6Co cemented carbides by hot oscillating pressing method. The investigation introduced the organization, hardness, and tensile properties of dissimilar joints using solid-state ultrasonic welding between Al5754-O and Ti-6Al-4V alloys with or without pure Al layers. The significant changes in microstructure were observed at the joint interface, where adhesion was more pronounced on both sides of joints with Al interlayer than in joints without interlayer [158]. Therefore, an asymmetric distribution of the hardness of the heterogeneous joints was observed resulting in a gradual increase of the hardness values from the Al side to the Ti side [159]. Khan et al. introduced the review analyses of friction stir riveting processes. The analysis also presented the ultrasonic welding of dissimilar alloys such as magnesium and titanium metals. A study of the thermo-mechanical analysis of the welding process with experimental and finite element methods was carried out. The magnesium alloy in the center of the welded joint partially melts and generates a liquid phase in a welding time of 0.5 s. Through finite element analysis, the friction coefficient of the Mg–Ti ultrasonic welding interface can be considered an average constant of 0.28 [160]. The maximum temperature at the interface can exceed 600°C to reach the melting point temperature of the magnesium alloy. The plastic deformation starts after 0.35 s and occurs on the magnesium side in the center of the interface [161].

3.4 Limitations of ultrasonic welding

This study was conducted to review previous research work and address future recommendations for ultrasonic welding of similar and dissimilar light metals together with light metals to other materials. Similarly, the objective of this review article is to provide a brief understanding of lightweight ultrasonic welding principle, current trends and research gap for follow on study. Table 1 presents the author's introduction, materials, optimized welding strength, and various process parameters studied for the ultrasonic welding of lightweight metals to lightweight metals. Moreover, Table 2 introduces the author's introduction, materials, optimized welding strength, and various process parameters studied for the ultrasonic welding of lightweight metals to other materials. In recent years, ultrasonic light alloy welding has developed rapidly due to its unique advantages. It is widely used in the automotive, electrical, battery, solar, and aerospace industries.

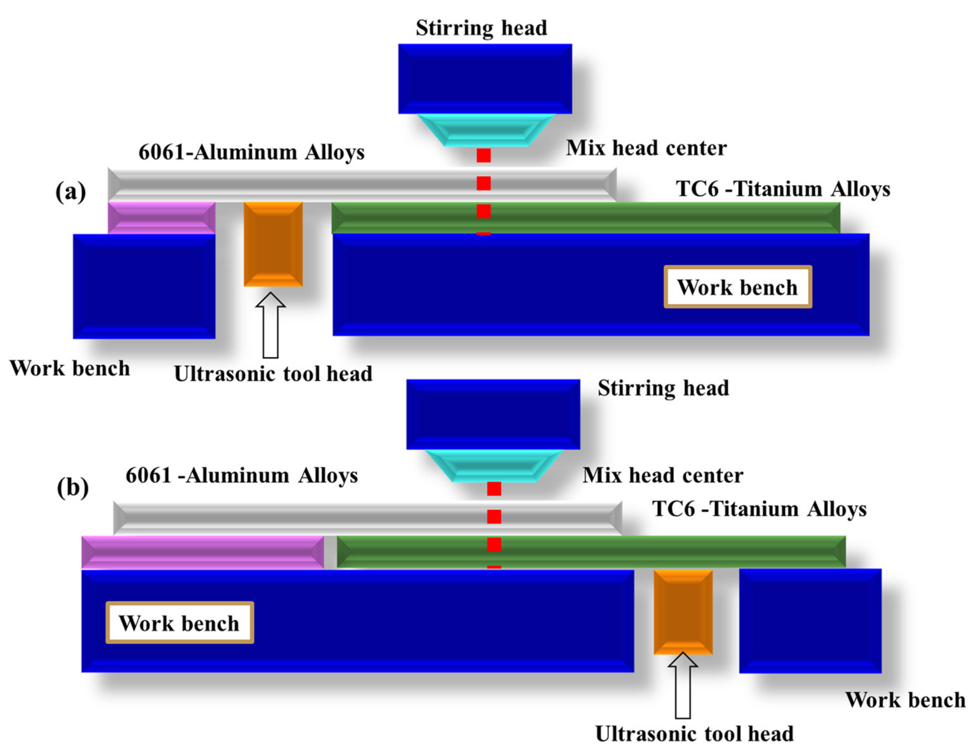

Figure 11: Schematic diagrams of the structure of Al/Ti Xenophilic and Xeno applied by ultrasound to the lower surface of titanium alloy: (a) Xenophilic FSLW and (b) Xeno FSLW.

Table 1: The author's introduction, materials, optimized welding strength, and various process parameters studied for the ultrasonic welding of lightweight metals to lightweight metals

Year	Author/reference	Material system	Factors studied	Welding energy	Weld time	Weld pressure/force	Knurling tooth angle	Amplitude	Frequency	Optimized weld strength
Ultrasonic welding of lightweight metals to lightweight metals										
2023	Zhao et al. [139]	Cu/Al	Effect of amplitude, welding time and clamping force	NA	380–600 ms	0.2–0.3 MPa	NA	22–30 µm	20 kHz	692.41 N
2023	Lun et al. [168]	TA1/Al	Effect of amplitude, welding time and shear strength	2,200 J	8 s	40 N	NA	70%	20 kHz	NA
2022	Tan et al. [169]	Al (AA2024)/Mg (AZ31B)	Effect of rotation speed, welding time and clamping force	NA	0.1 s	0.3 MPa	NA	25 µm	20 kHz	NA
2022	Ao et al. [170]	NiTi/Steel	Effect of surface morphology, interfacial microstructure and mechanism	750 J	0.1 s	0.4 MPa	NA	50 µm	20 kHz	690 N
2022	Lv et al. [171]	Al/Mg	Effect of vibration, frequency	NA	NA	300 MPa	NA	NA	20 kHz	NA
2021	Ma et al. [150]	Al/Ti	Effect of vibration	NA	0.3 s	300 MPa	NA	NA	NA	NA
2021	Shen et al. [2]	Ni/Cu	Effect of amplitude, welding energy, time and clamp pressure	600 J	0.1–0.5 s	4.2 bar	NA	8, 30 µm	20 kHz	3,200 N
2020	Abdi Behnagh et al. [172]	Al/Cu	Effect of frequency, clamp pressure, friction coefficient, and amplitude	NA	0.05 s	120 MPa	NA	25 µm	60 kHz	NA
2020	Du et al. [173]	Al/Steel	Effect of Knurling tooth angle and amplitude	NA	0.02–0.1 s	NA	110°–140°	24 µm	19 kHz	160 N
2019	Li and Cao [59]	Cu/Al	Effect of frequency, welding time and amplitude	NA	0.5 s	NA	NA	24 µm	20 kHz	2,175 N
2019	Huang et al. [174]	Mg/Mg	Effect of frequency, heat energy, and amplitude	500 J	0.33–0.1 s	0.3 MPa	NA	75 µm	20 kHz	NA
2019	Yang et al. [175]	Mg/Al	Effect of amplitude, welding energy, time and clamp pressure	1,000 J		0.276 MPa	NA	75 µm	20 kHz	2981.2 N
2019	Gu et al. [176]	Mg/Zn/Al	Effect of amplitude, welding energy, time and clamp pressure	1,400 J		0.4 MPa	NA	NA	20.11 kHz	NA
2019	Zhao et al. [160]	Mg/Ti	Effect of amplitude, welding time and clamping force	2,500 J	0.3–1.3 s	0.3 MPa	NA	75 µm	20 kHz	NA
2018	Nong et al. [11]	Ni/Cu	Effect of frequency, heat energy, and amplitude	600 J	0.3 s	70 psi	NA	20 µm	20 kHz	314.1 N
2018	Kumar et al. [177]	Al–Mg	Effect of vibration	NA	0.5 s	NA	NA	NA	NA	3,300 N
2018	Jedrasiak and Shercliff [178]	Al/Al	Effect of amplitude, welding energy, time, and clamp pressure	1,000 J	0.4 s	1 MPa	NA	5.5–6.5 µm	20.5 kHz	NA
2018	Patel et al. [179]	Al/SiC	Effect of Knurling tooth angle and amplitude	2,500 J	0.25–1.5 s	0.414 MPa	20°–100°	NA	20 kHz	4,300 N
2018	Liu et al. [113]	Cu/Al	Effect of amplitude, welding energy, time, and clamp pressure		0.4–1.2 s	NA	NA	20–25 µm	20 kHz	1,975 N

(Continued)

Table 1: *Continued*

Ultrasonic welding of lightweight metals to lightweight metals										
Year	**Author/reference**	**Material system**	**Factors studied**	**Welding energy**	**Weld time**	**Weld pressure/ force**	**Knurling tooth angle**	**Amplitude**	**Frequency**	**Optimized weld strength**
2015	Komiyama et al. [180]	Al/Al	Effect of frequency, heat energy, and amplitude	NA	3,000 ms	NA	NA	53 μm	15 kHz	588–882 N
2014	Zhang et al. [181]	Al/Ti	Effect of frequency, heat energy, and amplitude	2,000 J	0.6–1.4 s	0.55 MPa	NA	NA	20.5 kHz	3,500 N
2013	Shakil et al. [182]	Al/Steel	Effect of frequency, clamp pressure, friction coefficient, and amplitude	200 J	0.3 s	30–60 psi	NA	30–60 μm	20 kHz	500 N
2013	Lee et al. [183]	Cu/Al	Effect of frequency, clamp pressure, friction coefficient, and amplitude	400 J	500 ms	80 MPa	NA	24 μm	20 kHz	NA
2012	Panteli et al. [184]	Al/Mg	Effect of frequency, heat energy, strain deformation, and amplitude	600 J	0.4 s	NA	NA	5–6 μm	20.5 kHz	1,900 N
2011	Zhu et al. [141]	Ti/Al	Effect of amplitude, welding energy, time, and clamp pressure	NA	170 ms	0.4 MPa	NA	NA	20 kHz	NA
2011	Hajjari et al. [185]	Al/Mg	Effect of frequency, clamp pressure, friction coefficient, and amplitude	300 J	0.4 s	60 psi	NA	30 μm	20 kHz	1,500 N

Table 2: The author's introduction, materials, optimized welding strength, and various process parameters studied for the ultrasonic welding of lightweight metals to other materials

Ultrasonic welding of lightweight metals to other materials										
Year	**Author/ reference**	**Material system**	**Factors studied**	**Welding energy**	**Weld time**	**Weld pressure/ force**	**Knurling tooth angle**	**Amplitude**	**Frequency**	**Optimized weld strength**
2023	Balle et al. [33,39]	Al/CF	Effect of amplitude, welding time and shear strength	2,160 J	3.5 s	31.5 MPa	NA	38 and 42 μm	20 kHz	2,460 N
2022	Faudree et al. [186]	Ti/CF-epoxy	Effect of shear strength, mechanical, welding energy	1,800 J	0.3 ms	850 N	NA	65 μm	20 kHz	3,000 N
2021	Zeng et al. [187]	Al/CFRP	Effect of frequency, welding time, and shear strength	2,000 J	8.5 s	500 N	NA	60 μm	20 kHz	NA
2021	Lionetto et al. [188]	Al/CF epoxy	Effect of energy analysis and force	2,500 J	2.5 s	19 MPa	NA	30 μm	NA	280 N
2020	Dou et al. [189]	Al/PET	Effect of room temperature	36 J	500–800 ms	200 MPa	NA	40 μm	13.56 MHz	NA
2019	Staab and Balle [190]	Al/CFRP	Effect of rotation speed, welding time, and clamping force	4,300 J	0.1 s	300–400 N	NA	40 μm	20 kHz	8,310 N
2019	Li et al. [191]	Glass ribbon/Al ribbon	Effect of rotation speed, welding time, and clamping force	800 J	160 ms	723 N	NA	30 μm	35 kHz	NA
2019	Dal Conte et al. [29]	Al/CF/PA6	Effect of shear strength, mechanical, chemical, and physical treatments	3,000 J	500 ms	1.5 MPa	NA	34.5 μm	20 kHz	500 N
2018	Lionetto et al. [192]	Al/CF-epoxy	Effect of shear strength, mechanical, welding energy, clamping force	2,400 J	600 ms	283 MPa	NA	50 μm	20 kHz	280 N
2015	Yeh et al. [193]	Thermoplastic/Al	Effect of vibration, frequency	2,000 J	0.5 s	39 MPa	NA	80 μm	20 kHz	5,000 N
2014	Levy et al. [194]	Thermoplastic composites/metal	Effect of heat, efficiency	2,000 J	0.38 s	20 bar	NA	86.2 μm	20 kHz	NA

However, due to the complexity of the ultrasonic metal welding process, the mechanism of ultrasonic metal welding has not yet been unified with more understanding. Therefore, it will hinder the further development of ultrasonic welding applications of light alloys. Lately, the main limitation of the ultrasonic welding process is that it only works and joins with certain types of materials. In particular, it is limited to those materials that have a low melting point such as thermoplastics or thermosets. The ultrasonic welding process is also limited due to size, material properties, and time to complete the entire process [53,162–165]. Additionally, many metals cannot be welded using the ultrasonic welding method due to their high melting points. Similarly, hardness is also another barrier to joining dissimilar metals. The process parameters and setting time are currently considered the main factors limiting to obtain good welding results when joining dissimilar and dissimilar metals [166,167].

4 Conclusion

In this review article, we conducted a comprehensive literature survey, which identifies the potential of ultrasonic light alloy sheet welding. It discussed the benefits, challenges, and strategies, limitations and application scenarios for aluminum alloys, magnesium alloys and titanium alloys. The investigations have indicated that ultrasonic welding technology provides an ultra-fast and straightforward procedure for joining similar and dissimilar materials. This also provides ways to strengthen welded joints. The quality of ultrasonic welding has a significant impact on aluminum alloys, magnesium alloys and titanium alloys. The metal-to-metal joining review revealed that ultrasonic welding technology is cost-effective for the aerospace, automotive and aircraft industries. In addition, welding setup time is often considered the main parameter that affects welding quality and sometimes interrupts operations. Literature research shows that ultrasonic welding technology is an advantageous and significant method for joining light materials which produces soft, strong and crack-resistant joints.

4.1 Future research recommendations

Contemporary, a significant extent of research work has been conducted in the field of ultrasonic metal welding and the research is mainly limited to similar and dissimilar joints. There have not been enough research projects on building the integration of the static failure mechanism of ultrasonic welding. Furthermore, the literature review recommends the combination of ultrasonic metal welding with self-piercing rivets.

(1) Based on the ultrasonic metal welding process, the fatigue failure mechanism and crack failure mechanisms can be further investigated and industrialized.
(2) In order to promote the application of ultrasonic technology, future research in ultrasonic metal welding should be carried out in the following areas: Strengthening the fatigue performance of ultrasonic light alloy sheet welding and the failure of macro and micro studies, which is favorable for discovering the fatigue failure mechanism of the joint. For strength welding tests of alloy sheets with ultrasonic lightweight can be combined with numerical simulation that helps to reveal the principle of ultrasonic metal welding.
(3) Likewise, to strengthen the sandwich structure, the research of ultrasonic light alloy sheet welding is favorable for the expansion of ultrasonic metal welding in industrial application.
(4) Ultrasonic welding in wire harness still has research gap, and the stability of the welded joint can be further developed and strengthened.

Acknowledgments: The authors gratefully acknowledge postdoc start-up financial support from the Institute of Ultrasonic Technology, Shenzhen Polytechnic University (Grant Number: 6022331008K).

Funding information: This research is supported by National Natural Science Foundation of China (Grant No. 12104324); Postdoctoral Science Foundation of China (No. 2021M703392); Scientific Research Startup Fund for Shenzhen High-Caliber Personnel of SZPT (No. 6022310046K); Postdoctoral Startup Fund of Shenzhen Polytechnic University (No. 6021330001K and No. 6022331008K).

Author contributions: Conceptualization, L.Z., and Z.A.; Data curation, Z.A., and W.H.; Formal analysis, Z.A., and L.Z.; Investigation Z.A., and L.Z.; Methodology, Z.A.; Project administration, L.Z.; Resources, L.Z.; Software, Z.A., J.D., and W.H.; Supervision, L.Z.; Validation, Z.A., J.D., and S.W.; Writing – original draft, Z.A.; Writing – review & editing, Z.A., and L.Z. All authors have read and agreed to the published version of the manuscript.

Conflict of interest: The authors atate no conflict of interest.

Institutional review board statement: Not applicable.

Informed consent statement: Not applicable.

Data availability statement: Not applicable.

References

[1] Müller, F. W., C. Y. Chen, A. Schiebahn, and U. Reisgen. Application of electrical power measurements for process monitoring in ultrasonic metal welding. *Welding in the World*, Vol. 67, No. 2, 2023, pp. 395–415.

[2] Shen, N., A. Samanta, W. W. Cai, T. Rinker, B. Carlson, and H. Ding. 3D finite element model of dynamic material behaviors for multilayer ultrasonic metal welding. *Journal of Manufacturing Processes*, Vol. 62, No. August 2020, 2021, pp. 302–312.

[3] Brito, B. G., C. J. Teuwen, C. A. Dransfeld, and I. F. Villegas. The effects of misaligned adherends on static ultrasonic welding of thermoplastic composites. *Composites Part A: Applied Science and Manufacturing*, Vol. 155, No. November 2021, 2022, id. 106810.

[4] Kothuru, V. V. L., V. S. Sistla, I. H. Mohammed, and A. Jagana. Design and numerical analysis of rectangular sonotrode for ultrasonic welding. *Trends in Sciences*, Vol. 1911, 2022, pp. 1–14.

[5] Satpathy, M. P. and S. K. Sahoo. Experimental and numerical studies on ultrasonic welding of dissimilar metals. *International Journal of Advanced Manufacturing Technology*, Vol. 93, No. 5–8, 2017, pp. 2531–2545.

[6] Mostafavi, S., D. F. Hesser, and B. Markert. Detection of terminal oscillation pattern in ultrasonic metal welding. *Journal of Manufacturing Processes*, Vol. 41, April 2019, pp. 159–167.

[7] Zhao, D., W. Wang, D. Ren, and K. Zhao. Research on ultrasonic welding of copper wire harness and aluminum alloy: Based on experimental method and GA-ANN model. *Journal of Materials Research and Technology*, Vol. 22, 2023, pp. 3180–3191.

[8] Payão Filho, J. da. C., V. P. Maia, E. K. D. Passos, R. S. Gonzaga, and D. R. Julia. Probability of detection of discontinuities by ultrasonic phased array inspection of 9% Ni steel joints welded with alloy 625 as the filler metal. *Ultrasonics*, Vol. 119, No. August 2021, 2022, id. 106582.

[9] Du, Z., L. Duan, L. Jing, A. Cheng, and Z. He. Numerical simulation and parametric study on self-piercing riveting process of aluminium–steel hybrid sheets. *Thin-Walled Structures*, Vol. 164, April 2021, id. 107872.

[10] Selvaraj, S. K., K. Srinivasan, U. Chadha, R. Mishra, K. Arpit, K. Apurb, et al. Contemporary progresses in ultrasonic welding of aluminum metal matrix composites. *Frontiers in Materials*, Vol. 8, April 2021, pp. 1–13.

[11] Nong, L., C. Shao, T. H. Kim, and S. J. Hu. Improving process robustness in ultrasonic metal welding of lithium-ion batteries. *Journal of Manufacturing Systems*, Vol. 48, April 2018, pp. 45–54.

[12] Hoehr, L., J. Bavendiek, J. Sackmann, and W. K. Schomburg. Ultrasonic welding of polymer micro fluidic devices by inserting metal parts. *Microsystem Technologies*, Vol. 25, No. 2, 2019, pp. 673–681.

[13] Xie, J., Y. Chen, L. Yin, T. Zhang, S. Wang, and L. Wang. Microstructure and mechanical properties of ultrasonic spot welding TiNi/Ti6Al4V dissimilar materials using pure Al coating. *Journal of Manufacturing Processes*, Vol. 64, February 2021, pp. 473–480.

[14] Ni, Z. L., X. X. Wang, S. Li, and F. X. Ye. Mechanical strength enhancement of ultrasonic metal welded Cu/Cu joint by cu nanoparticles interlayer. *Journal of Manufacturing Processes*, Vol. 38, No. December 2018, 2019, pp. 88–92.

[15] Zhang, C., H. Li, Q. Liu, C. Huang, and K. Zhou. Ultrasonic Welding of Aluminum to Steel: A Review. *Metals*, Vol. 13, No. 1, 2023, pp. 1–22.

[16] Liu, L., D. Ren, and F. Liu. A review of dissimilar welding techniques for magnesium alloys to aluminum alloys. *Materials*, Vol. 7, No. 5, 2014, pp. 3735–3757.

[17] Jiang, H., G. Li, X. Zhang, and J. Cui. Fatigue and failure mechanism in carbon fiber reinforced plastics/aluminum alloy single lap joint produced by electromagnetic riveting technique. *Composites Science and Technology*, Vol. 152, 2017, pp. 1–10.

[18] Barimani-Varandi, A. and A. J. Aghchai. Electrically-assisted mechanical clinching of AA6061-T6 aluminum to galvanized DP590 steel: effect of geometrical features on material flow and mechanical strength. *Mechanics and Industry*, Vol. 21, No. 5, 2020, pp. 1–13.

[19] Das, A., I. Masters, and D. Williams. Process robustness and strength analysis of multi-layered dissimilar joints using ultrasonic metal welding. *International Journal of Advanced Manufacturing Technology*, Vol. 101, No. 1–4, 2019, pp. 881–900.

[20] Ramesh, M. and K. Panneerselvam. Optimization of Ultrasonic Welding Parameters Based on Response Surface Methodology. *Journal of Physics: Conference Series*, Vol. 2474, No. 1, id. 012029.

[21] Samir, S., K. Dave, V. Badheka, and D. Patel. Optimization of process parameters of ultrasonic metal welding for multi layers foil of AL8011 material. *Welding International*, Vol. 37, No. 3, 2023, pp. 1–14.

[22] Tsujino, J., T. Ueoka, K. Hasegawa, Y. Fujita, T. Shiraki, T. Okada, et al. New methods of ultrasonic welding of metal and plastic materials. *Ultrasonics*, Vol. 34, No. 2–5, 1996, pp. 177–185.

[23] Presse, J., B. Künkler, and T. Michler. Stress-based approach for fatigue life calculation of multi-material connections hybrid joined by self-piercing rivets and adhesive. *Thin-Walled Structures*, Vol. 159, No. August 2020, 2021, id. 107192.

[24] Cao, Y., Y. Zhang, W. Ming, W. He, and J. Ma. Review: The metal additive-manufacturing technology of the ultrasonic-assisted wire-and-arc additive-manufacturing process. *Metals*, Vol. 13, No. 2, 2023, pp. 1–23.

[25] Liu, Z., Y. Li, Z. Liu, Y. Yang, Y. Li, and Z. Luo. Ultrasonic welding of metal to fiber-reinforced thermoplastic composites: A review. *Journal of Manufacturing Processes*, Vol. 85, No. November 2022, 2023, pp. 702–712.

[26] Universio, T. P. *Ultrasonic Welding of Ceramic Metal, I*. Vol. 47. 1994, pp. 185–196.

[27] Lan, H. X., X. F. Gong, S. F. Zhang, L. Wang, B. Wang, and L. P. Nie. Ultrasonic vibration assisted tungsten inert gas welding of dissimilar metals 316L and L415. *International Journal of Minerals, Metallurgy and Materials*, Vol. 27, No. 7, 2020, pp. 943–953.

[28] Cheng, X. M., K. Yang, J. Wang, W. T. Xiao, and S. S. Huang. Ultrasonic system and ultrasonic metal welding performance: A status review. *Journal of Manufacturing Processes*, Vol. 84, October 2022, pp. 1196–1216.

[29] Dal Conte, U. F., I. F. Villegas, and J. Tachon. Ultrasonic plastic welding of CF/PA6 composites to aluminium: process and mechanical performance of welded joints. *Journal of Composite Materials*, Vol. 5318, 2019, pp. 2607–2621.

[30] Macwan, A., A. Kumar, and D. L. Chen. Ultrasonic spot welded 6111-T4 aluminum alloy to galvanized high-strength low-alloy steel: Microstructure and mechanical properties. *Materials and Design*, Vol. 113, 2017, pp. 284–296.

[31] Bahl, S., T. Singh, V. Kumar, S. Sehgal, and A. K. Bagha. A systematic review on recent progress in advanced joining techniques of the lightweight materials. *AIMS Materials Science*, Vol. 8, No. 1, 2021, pp. 62–81.

[32] Singh, R. P., S. Dubey, A. Singh, and S. Kumar. A Review paper on friction stir welding process. *Materials Today: Proceedings*, Vol. 38, 2020, pp. 6–11.

[33] Ragupathi, B., M. F. Bacher, and F. Balle. First efforts on recovery of thermoplastic composites at low temperatures by power ultrasonics. *Cleaner Materials*, Vol. 8, March 2023, id. 100186.

[34] Hunedoara, F. E., I. Journal, E. T. Xv, E. Hunedoara, T. Nguyenvo, and P. Lenfeld. A review of studies on ultrasonic welding. *International Journal of Advance Engineering and Research Development*, Vol. 4, No. 09, 2017, pp. 1–14.

[35] Tilahun, S., M. D. Vijayakumar, C. Ramesh Kannan, S. Manivannan, J. Vairamuthu, K. P. Manoj Kumar. A review on ultrasonic welding of various materials and their mechanical properties. *IOP Conference Series: Materials Science and Engineering*, Vol. 988, No. 1, 2020, pp. 1–17.

[36] Ulutaş, A. Joining Techniques Like Welding in Lightweight Material Structures. IGI Global, Balıkesir University, Turkey, 2021, pp. 1–121.

[37] Lopes, J. G. and J. P. Oliveira. A short review on welding and joining of high entropy alloys. *Metals*, Vol. 10, No. 2, 2020, pp. 1–21.

[38] Bhudolia, S. K., G. Gohel, K. F. Leong, and A. Islam. Advances in ultrasonicwelding of thermoplastic composites: A review. *Materials*, Vol. 13, No. 6, 2020, pp. 1–18.

[39] Li, J., J. Zillner, and F. Balle. In-depth evaluation of ultrasonically welded al/cu joint: plastic deformation, microstructural evolution, and correlation with mechanical properties. *Materials*, Vol. 16, No. 8, 2023, id. 3033.

[40] Li, Z., Z. Huang, F. Sun, X. Li, and J. Ma. Forming of metallic glasses: Mechanisms and processes. *Materials Today Advances*, Vol. 7, 2020, pp. 1–16.

[41] Unnikrishnan, T. G. and P. Kavan. A review study in ultrasonic-welding of similar and dissimilar thermoplastic polymers and its composites. *Materials Today: Proceedings*, Vol. 56, 2022, pp. 3294–3300.

[42] Kim, T. H., J. Yum, S. J. Hu, J. P. Spicer, and J. A. Abell. Process robustness of single lap ultrasonic welding of thin, dissimilar materials. *CIRP Annals - Manufacturing Technology*, Vol. 60, No. 1, 2011, pp. 17–20.

[43] Wang, Y., W. Tao, and S. Yang. A method for improving joint strength of resistance spot welds of AA 5182-O aluminum alloy. *Journal of Manufacturing Processes*, Vol. 45, March 2019, pp. 661–669.

[44] Ren, D., D. Zhao, C. Li, L. Liu, and K. Zhao. Resistance ceramic-filled annular welding of thin steel sheets. *Journal of Manufacturing Processes*, Vol. 45, April 2019, pp. 588–594.

[45] Paidar, M., O. O. Ojo, A. Moghanian, A. S. Karapuzha, and A. Heidarzadeh. Modified friction stir clinching with protuberance-keyhole levelling: A process for production of welds with high strength. *Journal of Manufacturing Processes*, Vol. 41, March 2019, pp. 177–187.

[46] Ji, H., J. Wang, and M. Li. Evolution of the bulk microstructure in 1100 aluminum builds fabricated by ultrasonic metal welding. *Journal of Materials Processing Technology*, Vol. 214, No. 2, 2014, pp. 175–182.

[47] de Leon, M. and H. S. Shin. Weldability assessment of Mg alloy (AZ31B) sheets by an ultrasonic spot welding method. *Journal of Materials Processing Technology*, Vol. 243, 2017, pp. 1–8.

[48] Kim, J., J. Kim, I. J. Kim, S. Kang, and K. Chun. An analysis of mechanical properties for ultrasonicallywelded multiple C1220-Al1050 layers. *Applied Sciences (Switzerland)*, Vol. 9, No. 19, 2019, pp. 1–24.

[49] Kim, J., J. Kim, and I. Kim. Analysis of welding properties using various horn-tip patterns in the ultrasonic metal welding process. *Mechanics and Industry*, Vol. 21, No. 1, 2020, pp. 1–9.

[50] Parmar, U. and D. H. Pandya. Experimental investigation of ultrasonic welding on non-metallic material. *Procedia Technology*, Vol. 23, 2016, pp. 551–557.

[51] Charlier, Q., J. Viguié, B. Harthong, J. B. Toni, M. Terrien, D. Imbault, et al. Experimental investigation and process optimization of the ultrasonic welding applied to papers. *Materialwissenschaft und Werkstofftechnik*, Vol. 52, No. 8, 2021, pp. 891–906.

[52] Schubert, A., H. Zeidler, S. F. Jahn, S. Flemmig, and R. Schulze. Vibration analysis of an ultrasonic-assisted joining system. *Procedia Engineering*, Vol. 69, 2014, pp. 1021–1028.

[53] Tsiangou, E., S. Teixeira de Freitas, I. F. Villegas, and R. Benedictus. Ultrasonic welding of epoxy- to polyetheretherketone- based composites: investigation on the material of the energy director and the thickness of the coupling layer. *Journal of Composite Materials*, Vol. 54, No. 22, 2020, pp. 3081–3098.

[54] Jongbloed, B., J. Teuwen, G. Palardy, I. Fernandez Villegas, and R. Benedictus. Continuous ultrasonic welding of thermoplastic composites: enhancing the weld uniformity by changing the energy director. *Journal of Composite Materials*, Vol. 54, No. 15, 2020, pp. 2023–2035.

[55] Wei, L. S., X. X. Zhang, M. F. Qian, P. G. Martin, L. Geng, T. B. Scott, et al. Compressive deformation of polycrystalline Ni-Mn-Ga alloys near chemical ordering transition temperature. *Materials and Design*, Vol. 142, 2018, pp. 329–339.

[56] Bagheri, B., M. Alizadeh, S. E. Mirsalehi, A. Shamsipur, and A. Abdollahzadeh. The effect of rotational speed and dwell time on Al/SiC/Cu composite made by friction stir spot welding. *Welding in the World*, Vol. 66, No. 11, 2022, pp. 2333–2350.

[57] Boucherit, A., S. Abdi, M. Aissani, B. Mehdi, K. Abib, and R. Badji. Weldability, microstructure, and residual stress in Al/Cu and Cu/Al friction stir spot weld joints with Zn interlayer. *International Journal of Advanced Manufacturing Technology*, Vol. 111, No. 5–6, 2020, pp. 1553–1569.

[58] Liu, J., S. Niu, R. Ren, S. Ji, L. Wang, and Z. Lv. Improving joint morphologies and tensile strength of Al/Mg dissimilar alloys friction stir lap welding by changing Zn Interlayer thickness. *Acta Metallurgica Sinica (English Letters)*, Vol. 32, No. 11, 2019, pp. 1385–1395.

[59] Li, H. and B. Cao. Effects of welding pressure on high-power ultrasonic spot welding of Cu/Al dissimilar metals. *Journal of Manufacturing Processes*, Vol. 46, September 2019, pp. 194–203.

[60] Rousseau, J. N., A. Bois-Brochu, N. Giguère, and C. Blais. Study of ultrasonic additive manufacturing and its utilization for the production of aluminum components made of alloys of the AA5XXX series. *International Journal of Advanced Manufacturing Technology*, Vol. 119, No. 11–12, 2022, pp. 7983–8002.

[61] Li, Y., D. Fan, Y. P. Li, J. K. Huang, and X. Q. Yu. Effect of ultrasonic power on microstructural and mechanical properties of Al/Cu plasma Arc welding–brazing joints. *Journal of Materials Engineering and Performance*, Vol. 28, 2022, pp. 168–177.

[62] Kumar, S., C. Wu, and L. Shi. Intermetallic diminution during friction stir welding of dissimilar Al/Mg alloys in lap configuration via ultrasonic assistance. *Metallurgical and Materials Transactions A: Physical Metallurgy and Materials Science*, Vol. 51, No. 11, 2020, pp. 5725–5742.

[63] Ni, Z. L. and F. X. Ye. Dissimilar joining of aluminum to copper using ultrasonic welding. *Materials and Manufacturing Processes*, Vol. 31, No. 16, 2016, pp. 2091–2100.
[64] Kah, P., C. Vimalraj, J. Martikainen, and R. Suoranta. Factors influencing Al-Cu weld properties by intermetallic compound formation. *International Journal of Mechanical and Materials Engineering*, Vol. 10, No. 1, 2015, pp. 1–13.
[65] Satpathy, M. P. and S. K. Sahoo. Microstructural and mechanical performance of ultrasonic spot welded Al-Cu joints for various surface conditions. *Journal of Manufacturing Processes*, Vol. 22, 2016, pp. 108–114.
[66] Satpathy, M. P. and S. K. Sahoo. Mechanical performance and metallurgical characterization of ultrasonically welded dissimilar joints. *Journal of Manufacturing Processes*, Vol. 25, 2017, pp. 443–451.
[67] Huang, L., J. Bonnen, J. Lasecki, H. Guo, and X. Su. Fatigue and fretting of mixed metal self-piercing riveted joint. *International Journal of Fatigue*, Vol. 83, 2016, pp. 230–239.
[68] Li, D., L. Han, M. Thornton, M. Shergold, and G. Williams. The influence of fatigue on the stiffness and remaining static strength of self-piercing riveted aluminium joints. *Materials and Design*, Vol. 54, 2014, pp. 301–314.
[69] Zou, M., Z. Ge, L. Qi, X. Zhou, X. Wei, J. Zhang, et al. Effect of Erbium (Er) on the hot cracking behaviour of Al-5Cu Alloy. *Materials Science and Technology (United Kingdom)*, Vol. 3817, 2022, pp. 1501–1509.
[70] Balasundaram, R., V. K. Patel, S. D. Bhole, and D. L. Chen. Effect of zinc interlayer on ultrasonic spot welded aluminum-to-copper joints. *Materials Science and Engineering A*, Vol. 607, 2014, pp. 277–286.
[71] Patel, V. K., D. L. Chen, and S. D. Bhole. Dissimilar ultrasonic spot welding of Mg-Al and Mg-High strength low alloy steel. *Theoretical and Applied Mechanics Letters*, Vol. 4, No. 4, 2014, id. 041005.
[72] Patel, V. K., S. D. Bhole, and D. L. Chen. Ultrasonic spot welding of lightweight alloys. *13th International Conference on Fracture 2013, ICF 2013*, 1, May 2013, pp. 30–39.
[73] Chen, Y., Y. Li, L. Shi, C. Wu, S. Li, and S. Gao. Optimizing the shoulder diameter for double side friction stir welding of medium-thick TC4/AA2024 dissimilar alloys by taguchi optimization technique. *Welding in the World*, Vol. 67, No. 8, 2023, pp. 1887–1899.
[74] Ebrahimpour, A., A. Shakoori, and T. Saeid. Metallurgical and mechanical study of the effect of FSW parameters on dissimilar joining of St37 and AZ31. *Welding in the World*, Vol. 67, 2023, pp. 2683–2702.
[75] Karkhin, V. A., V. V. Plochikhine, A. S. Ilyin, and H. W. Bergmann. Inverse modelling of fusion welding processes. *Welding in the World*, Vol. 46, No. 11–12, 2002, pp. 2–13.
[76] Karkhin, V. A., A. S. Ilin, H. J. Pesen, A. A. Prikhodovsky, V. V. Plochikhine, M. V. Makhutin, et al. Effects of latent heat of fusion on thermal processes in laser welding of aluminium alloys. *Science and Technology of Welding and Joining*, Vol. 10, No. 5, 2005, pp. 597–603.
[77] Araujo, L. C., P. V. S. Machado, M. V. S. Pereira, and J. A. Araújo. An alternative approach to calibrate multiaxial fatigue models of steels with small defects. *Procedia Structural Integrity*, Vol. 19, 2019, pp. 19–26.
[78] Touileb, K., A. Ouis, A. C. Hedhibi, A. Ibrahim, and H. S. Abdo. Effects of metal and fluoride powders deposition on hot-cracking susceptibility of 316L stainless steel in TIG welding. *Metals*, Vol. 12, No. 7, 2022, pp. 1–15.
[79] Ploshikhin, V., A. Prihodovsky, and A. Ilin. Experimental investigation of the hot cracking mechanism in welds on the microscopic scale. *Frontiers of Materials Science*, Vol. 5, No. 2, 2011, pp. 135–145.
[80] Zhao, L., X. He, B. Xing, X. Zhang, C. Deng, and Y. Liu. Fracture mechanism of titanium sheet self-piercing riveted joints. *Thin-Walled Structures*, Vol. 144, January 2019, id. 106353.
[81] Tutunjian, S., O. Eroglu, M. Dannemann, N. Modler, and F. Fischer. A numerical analysis of an energy directing method through friction heating during the ultrasonic welding of thermoplastic composites. *Journal of Thermoplastic Composite Materials*, Vol. 33, No. 11, 2020, pp. 1569–1587.
[82] Villegas, I. F. and G. Palardy. Ultrasonic welding of CF/PPS composites with integrated triangular energy directors: melting, flow and weld strength development. *Composite Interfaces*, Vol. 24, No. 5, 2017, pp. 515–528.
[83] Tutunjian, S., M. Dannemann, F. Fischer, O. Eroğlu, and N. Modler. A control method for the ultrasonic spot welding of fiber-reinforced thermoplastic laminates through the weld-power time derivative. *Journal of Manufacturing and Materials Processing*, Vol. 3, No. 1, 2019, pp. 1–17.
[84] Jongbloed, B., J. Teuwen, R. Benedictus, and I. F. Villegas. On differences and similarities between static and continuous ultrasonic welding of thermoplastic composites. *Composites Part B: Engineering*, Vol. 203, October 2020, id. 108466.
[85] Fernandez Villegas, I., B. Valle Grande, H. E. N. Bersee, and R. Benedictus. a comparative evaluation between flat and traditional energy directors for ultrasonic welding of CF/PPS thermoplastic composites. *Composite Interfaces*, Vol. 22, No. 8, 2015, pp. 717–729.
[86] Regazzi, A., J. Viguié, B. Harthong, P. J. J. Dumont, D. Imbault, R. Peyroux, et al. Ultrasonic welding of 100% lignocellulosic papers. *Journal of Materials Science*, Vol. 54, No. 19, 2019, pp. 12938–12950.
[87] Palardy, G. and I. F. Villegas. On the effect of flat energy directors thickness on heat generation during ultrasonic welding of thermoplastic composites. *Composite Interfaces*, Vol. 24, No. 2, 2017, pp. 203–214.
[88] Mustafa, S. E., R. N. Rai, and R. Firoz. Enhancement of joint properties and reduction of intermetallics in FSW of highly dissimilar Al/Ti alloys. *Welding in the World*, Vol. 67, No. 6, 2023, pp. 1393–1410.
[89] Li, W., J. Huan Chang, B. Feng Wen, and R. Cao. Joining of dissimilar metals between magnesium AZ31B and aluminum A6061-T6 using galvanized steel as a transition joining layer. *Journal of Iron and Steel Research International*, Vol. 29, No. 4, 2022, pp. 677–686.
[90] Liu, Z., S. Ji, and X. Meng. Joining of magnesium and aluminum alloys via ultrasonic assisted friction stir welding at low temperature. *International Journal of Advanced Manufacturing Technology*, Vol. 97, No. 9–12, 2018, pp. 4127–4136.
[91] Shi, X. F., L. Z. Chang, Z. H. Zhu, J. J. Wang, and L. Zhou. Effect of noncontact ultrasonic technology on solidification quality of electroslag steel. *Journal of Iron and Steel Research International*, Vol. 23, No. 11, 2016, pp. 1168–1176.
[92] Lakshminarayanan, A. K., K. Shanmugam, and V. Balasubramanian. Effect of welding processes on tensile and impact properties, hardness and microstructure of AISI 409M ferritic stainless joints fabricated by duplex stainless steel filler

metal. *Journal of Iron and Steel Research International*, Vol. 16, No. 5, 2009, pp. 66–72.
[93] Azéma, A., F. Angelini, B. Mille, G. Framezelle, and D. Chauveau. Ultrasonic phased array contribution to the knowledge of the flow fusion welding process used to make the roman large bronze statues. *Welding in the World*, Vol. 57, No. 4, 2013, pp. 477–486.
[94] Majeed, T., Y. Mehta, and A. N. Siddiquee. Al alloy tailor welded blank fabrication by friction stir welding: Effect of double-pass. *Journal of Materials Engineering and Performance*, Vol. 31, No. 1, 2022, pp. 410–423.
[95] Liu, Y., J. Bi, and D. Yang. Microstructure and mechanical properties of refill friction stir spot welded 6005 Al alloy butt joints. *Jom*, Vol. 74, No. 7, 2022, pp. 2838–2845.
[96] Gester, A., G. Wagner, P. Pöthig, J. P. Bergmann, and M. Fritzsche. Analysis of the oscillation behavior during ultrasonic welding of EN AW-1070 wire strands and EN CW004A terminals. *Welding in the World*, Vol. 66, No. 3, 2022, pp. 567–576.
[97] Hopmann, C., R. Dahlmann, M. Weihermüller, J. Wipperfürth, and J. Sommer. Determination of the frequency- and temperature-dependent stiffness and damping properties of thermoplastics for the prediction of the vibration and heating behaviour during ultrasonic welding. *Welding in the World*, Vol. 67, No. 2, 2023, pp. 435–445.
[98] Pöthig, P., M. Grätzel, and J. P. Bergmann. Influence of different surface conditions on mechanical properties during ultrasonic welding of aluminum wire strands and copper terminals. *Welding in the World*, Vol. 67, 2023, p. 1427–1436.
[99] Regensburg, A., F. Petzoldt, R. Schürer, P. Hellwig, and J. P. Bergmann. Effect of local preheating during ultrasonic welding of Al-Cu joints on strand compaction and bond formation. *Welding in the World*, Vol. 61, No. 3, 2017, pp. 443–451.
[100] Abbas, N., Z. Abbas, and X. Liu. Adaptive recursive sliding mode control (ARSMC)-Based UAV control for future smart cities. *Applied Sciences*, Vol. 13, No. 11, 2023, pp. 1–19.
[101] Abbas, N., Z. Abbas, X. Liu, S. S. Khan, E. D. Foster, and S. Larkin. A survey: future smart cities based on advance control of Unmanned Aerial Vehicles (UAVs). *Applied Sciences (Switzerland)*, Vol. 13, No. 17, 2023, pp. 1–26.
[102] Ragavendran, M. and M. Vasudevan. Effect of laser and hybrid laser welding processes on the residual stresses and distortion in AISI Type 316L(N) stainless steel weld joints. *Metallurgical and Materials Transactions B: Process Metallurgy and Materials Processing Science*, Vol. 52, No. 4, 2021, pp. 2582–2603.
[103] Tarasov, S. Y., A. V. Vorontsov, S. V. Fortuna, V. E. Rubtsov, V. A. Krasnoveikin, and E. A. Kolubaev. Ultrasonic-assisted laser welding on AISI 321 stainless steel. *Welding in the World*, Vol. 63, No. 3, 2019, pp. 875–886.
[104] Elsheikh, A. H., M. Abd Elaziz, and A. Vendan. Modeling ultrasonic welding of polymers using an optimized artificial intelligence model using a gradient-based optimizer. *Welding in the World*, Vol. 66, No. 1, 2022, pp. 27–44.
[105] Ben Khalifa, A., S. Braiek, A. Fradj, and M. Trigui. Experimental investigation of joints strength obtained by ultrasonic welding and soldering under pure T-Peel tests using DIC. *Welding in the World*, Vol. 67, No. 2, 2023, pp. 495–511.
[106] Gorunov, A. I., O. A. Nyukhlaev, and A. K. Gilmutdinov. Investigation of microstructure and properties of low-carbon steel during ultrasonic-assisted laser welding and cladding. *International Journal of Advanced Manufacturing Technology*, Vol. 99, No. 9–12, 2018, pp. 2467–2479.
[107] Zhi, Q., J. M. Ma, X. R. Tan, Z. X. Liu, Z. G. Tian, and P. C. Wang. Single-sided ultrasonic welding of carbon fiber/Nylon 66 composite. *Welding in the World*, Vol. 65, No. 10, 2021, pp. 2047–2058.
[108] Li, H., C. Chen, R. Yi, Y. Li, and J. Wu. Ultrasonic welding of fiber-reinforced thermoplastic composites: A review. *International Journal of Advanced Manufacturing Technology*, Vol. 120, No. 1–2, 2022, pp. 29–57.
[109] Ma, Q., H. Chen, N. Ren, Y. Zhang, L. Hu, W. Meng, et al. Effects of ultrasonic vibration on microstructure, mechanical properties, and fracture mode of inconel 625 parts fabricated by cold metal transfer arc additive manufacturing. *Journal of Materials Engineering and Performance*, Vol. 30, No. 9, 2021, pp. 6808–6820.
[110] Hopmann, C. and A. van Aaken. Ultrasonic welding of polyamide —influence of moisture on the process relevant material properties. *Welding in the World*, Vol. 58, No. 6, 2014, pp. 787–793.
[111] Baradarani, F., S. Emami, A. Mostafapour, and F. K. Md. Influence of ultrasonic vibration on the microstructure and texture evolution of AZ91 magnesium alloy during ultrasonic-assisted friction stir welding. *Welding in the World*, Vol. 6512, 2021, pp. 2371–2382.
[112] Wu, C. Y., A. Benatar, and A. Mokhtarzadeh. Comparison of ultrasonic welding and vibration welding of thermoplastic polyolefin. *Welding in the World*, Vol. 56, No. 1–2, 2012, pp. 69–75.
[113] Liu, J., B. Cao, and J. Yang. Modelling intermetallic phase growth during high-power ultrasonic welding of copper and aluminum. *Journal of Manufacturing Processes*, Vol. 35, September 2018, pp. 595–603.
[114] Lu, Y., H. Song, G. A. Taber, D. R. Foster, G. S. Daehn, and W. Zhang. In-situ measurement of relative motion during ultrasonic spot welding of aluminum alloy using photonic doppler velocimetry. *Journal of Materials Processing Technology*, Vol. 231, 2016, pp. 431–440.
[115] Bakavos, D. and P. B. Prangnell. Mechanisms of joint and microstructure formation in high power ultrasonic spot welding 6111 aluminium automotive sheet. *Materials Science and Engineering A*, Vol. 527, No. 23, 2010, pp. 6320–6334.
[116] He, B., H. Deng, M. Jiang, K. Wei, and L. Li. Effect of ultrasonic impact treatment on the ultra high cycle fatigue properties of SMA490BW steel welded joints. *International Journal of Advanced Manufacturing Technology*, Vol. 96, No. 5–8, 2018, pp. 1571–1577.
[117] Milewski, A., P. Kluk, W. Kardyś, and P. Kogut. Modelling and designing of ultrasonic welding systems. *Archives of Acoustics*, Vol. 40, No. 1, 2015, pp. 93–99.
[118] Lee, S. S., T. H. Kim, S. J. Hu, W. W. Cai, and J. A. Abell. Analysis of weld formation in multilayer ultrasonic metal welding using high-speed images. *Journal of Manufacturing Science and Engineering, Transactions of the ASME*, Vol. 137, No. 3, 2015, pp. 1–8.
[119] Haddadi, F., D. Strong, and P. B. Prangnell. Effect of zinc coatings on joint properties and interfacial reactions in aluminum to steel ultrasonic spot welding. *Jom*, Vol. 64, No. 3, 2012, pp. 407–413.
[120] Haddadi, F. and F. Abu-Farha. Microstructural and mechanical performance of aluminium to steel high power ultrasonic spot welding. *Journal of Materials Processing Technology*, Vol. 225, No. June 2015, 2015, pp. 262–274.
[121] Mirza, F. A., A. Macwan, S. D. Bhole, and D. L. Chen. Fatigue behavior of ultrasonic spot welded similar aluminum 5754 alloy. International Conference on Innovative Technologies, Dubrovnik, Croatia, Vol. 5, 2015, pp. 9–12.
[122] Ni, Z. L. and F. X. Ye. Weldability and Mechanical Properties of Ultrasonic Welded Aluminum to Nickel Joints. *Materials Letters*, Vol. 185, 2016, pp. 204–207.

[123] Shin, H. S. and M. De Leon. Parametric study in similar ultrasonic spot welding of A5052-H32 alloy sheets. *Journal of Materials Processing Technology*, Vol. 224, 2015, pp. 222–232.

[124] Peng, H., D. Chen, and X. Jiang. Microstructure and mechanical properties of an ultrasonic spot welded aluminum alloy: The effect of welding energy. *Materials*, Vol. 10, No. 5, 2017, pp. 3245–3257.

[125] Mirza, F. A., A. Macwan, S. D. Bhole, and D. L. Chen. Microstructure and fatigue properties of ultrasonic spot welded joints of aluminum 5754 alloy. *Jom*, Vol. 68, No. 5, 2016, pp. 1465–1475.

[126] Dhara, S. and A. Das. Impact of ultrasonic welding on multi-layered Al–Cu joint for electric vehicle battery applications: A layer-wise microstructural analysis. *Materials Science and Engineering A*, Vol. 791, 2020, id. 139795.

[127] Liu, J., B. Cao, and J. Yang. Texture and intermetallic compounds of the Cu/Al dissimilar joints by high power ultrasonic welding. *Journal of Manufacturing Processes*, Vol. 76, February 2022, pp. 34–45.

[128] Al-Sarraf, Z. and M. Lucas. A study of weld quality in ultrasonic spot welding of similar and dissimilar metals. *Journal of Physics: Conference Series*, Vol. 382, No. 1, 2012, pp. 1–7.

[129] Jasmin, N. M., K. A. S. Lewise, D. Raguraman, M. Murugan, S. S. V. S. Aditya, T. S. A. Reddy, et al. An overview on characteristics and performance of ultrasonic welding process on different materials. *Materials Today: Proceedings*, Vol. 50, 2021, pp. 1508–1510.

[130] Macwan, A. and D. L. Chen. Ultrasonic spot welding of a rare-earth containing ZEK100 magnesium alloy: effect of welding. *Energy Metallurgical and Materials Transactions A: Physical Metallurgy and Materials Science*, Vol. 47, No. 4, 2016, pp. 1686–1697.

[131] Arghavani, M. R., M. Movahedi, and A. H. Kokabi. Role of zinc layer in resistance spot welding of aluminium to steel. *Materials and Design*, Vol. 102, 2016, pp. 106–114.

[132] Čiripová, L., L. Falat, V. Homolová, M. Džupon, R. Džunda, and I. Dlouhỳ. The effect of electrolytic hydrogenation on mechanical properties of T92 steel weldments under different PWHT conditions. *Materials*, Vol. 13, No. 16, 2020, pp. 1–20.

[133] Ji, S., S. Niu, and J. Liu. Dissimilar Al/Mg alloys friction stir lap welding with Zn foil assisted by ultrasonic. *Journal of Materials Science and Technology*, Vol. 35, No. 8, 2019, pp. 1712–1718.

[134] Wang, C., Y. Xing, J. Hu, J. Luo, and S. Zeng. Investigation on mechanism of ultrasonic welding AZ31B/5052 joint with laser texturing on mental surface. *International Journal of Advanced Manufacturing Technology*, Vol. 122, No. 1, 2022, pp. 159–171.

[135] Fujii, H. T., H. Endo, Y. S. Sato, and H. Kokawa. Interfacial microstructure evolution and weld formation during ultrasonic welding of Al Alloy to Cu. *Materials Characterization*, Vol. 139, March 2018, pp. 233–240.

[136] Prangnell, P., F. Haddadi, and Y. C. Chen. Ultrasonic spot welding of aluminium to steel for automotive applications-microstructure and optimisation. *Materials Science and Technology*, Vol. 27, No. 3, 2011, pp. 617–624.

[137] Pati, P. R., M. P. Satpathy, A. Pattanaik, S. K. Mohapatra, and S. B. Mishra. Ultrasonic spot welding of Al/Mg alloys: A state-of-the-art review. *Materials Today: Proceedings*, Vol. 33, 2020, pp. 4981–4987.

[138] Zhao, D., K. Zhao, D. Ren, and X. Guo. Ultrasonic welding of magnesium-titanium dissimilar metals: A study on influences of welding parameters on mechanical property by experimentation and artificial neural network. *Journal of Manufacturing Science and Engineering, Transactions of the ASME*, Vol. 139, No. 3, 2017, pp. 1–9.

[139] Zhao, D., C. Jiang, and K. Zhao. Ultrasonic welding of AZ31B magnesium alloy and pure copper: microstructure, mechanical properties and finite element analysis. *Journal of Materials Research and Technology*, Vol. 23, 2023, pp. 1273–1284.

[140] Aubert and Duval. *Titanium Alloy Ti5553*. Fondation Aubert & Duval s'attache à encourager, Located in All European countries, pp. 3–4.

[141] Zhu, Z., K. Y. Lee, and X. Wang. Ultrasonic welding of dissimilar metals, AA6061 and Ti6Al4V. *International Journal of Advanced Manufacturing Technology*, Vol. 59, No. 5–8, 2012, pp. 569–574.

[142] Zhou, L., J. Min, W. X. He, Y. X. Huang, and X. G. Song. Effect of welding time on microstructure and mechanical properties of Al-Ti ultrasonic spot welds. *Journal of Manufacturing Processes*, Vol. 33, April 2018, pp. 64–73.

[143] Lu, S., D. Wu, M. Yan, and R. Chen. Achieving high-strength and toughness in a Mg-Gd-Y alloy using multidirectional impact forging. *Materials*, Vol. 15, No. 4, 2022, pp. 1–12.

[144] Osipovich, K., K. Kalashnikov, A. Chumaevskii, D. Gurianov, T. Kalashnikova, A. Vorontsov, et al. Wire-feed electron beam additive manufacturing: A review. *Metals*, Vol. 13, No. 2, 2023, pp. 1–37.

[145] Gao, T., K. Wang, Z. Ling, and Z. Wang. Effect of a compound energy field with temperature and ultrasonic vibration on the material properties and bending process of TC2 Titanium alloy. *Materials*, Vol. 14, No. 23, 2021, pp. 1–22.

[146] Zhang, C., J. D. Robson, S. J. Haigh, and P. B. Prangnell. Interfacial segregation of alloying elements during dissimilar ultrasonic welding of AA6111 aluminum and Ti6Al4V titanium. *Metallurgical and Materials Transactions A: Physical Metallurgy and Materials Science*, Vol. 50, No. 11, 2019, pp. 5143–5152.

[147] Zhang, C., D. Wu, Y. He, W. Pan, J. Wang, and E. Han. Twinning Behavior, microstructure evolution and mechanical property of random-orientated ZK60 Mg alloy compressed at room temperature. *Materials*, Vol. 16, No. 3, 2023 Jan, id. 1163.

[148] Liu, Y., Z. Liu, G. Zhou, C. He, and J. Zhang. Microstructures and properties of Al-Mg alloys manufactured by WAAM-CMT. *Materials*, Vol. 15, No. 15, 2022, pp. 1–18.

[149] Shalomeev, V., G. Tabunshchyk, V. Greshta, K. Korniejenko, M. D. Guigou, and S. Parzych. Casting welding from magnesium alloy using filler materials that contain scandium. *Materials*, Vol. 15, No. 12, 2022, pp. 1–11.

[150] Ma, Z., X. Sun, S. Ji, Y. Wang, and Y. Yue. Influences of ultrasonic on friction stir welding of Al/Ti dissimilar alloys under different welding conditions. *International Journal of Advanced Manufacturing Technology*, Vol. 112, No. 9–10, 2021, pp. 2573–2582.

[151] Hu, W., Q. Li, Y. Wang, W. Bai, Z. Liang, and D. Yan. Effect of welding parameters on microstructure and mechanical properties of friction-stir-welded Al-Mg-Si alloy. *Journal of Materials Engineering and Performance*, Vol. 29, No. 2, 2020, pp. 866–876.

[152] Song, Q., Z. W. Ma, S. De Ji, Q. H. Li, L. F. Wang, and R. Li. Influence of pin offset on microstructure and mechanical properties of friction stir welded Mg/Ti dissimilar alloys. *Acta Metallurgica Sinica (English Letters)*, Vol. 32, No. 10, 2019, pp. 1261–1268.

[153] Hong, K., Y. Wang, J. Zhou, C. Zhou, and L. Wang. Investigation on ultrasonic assisted friction stir welding of aluminum/steel dissimilar alloys. *High Temperature Materials and Processes*, Vol. 40, No. 1, 2021, pp. 45–52.

[154] Zhou, X., J. Duan, F. Zhang, and S. Zhong. The Study on mechanical strength of titanium-aluminum dissimilar butt joints by laser welding-brazing process. *Materials*, Vol. 12, No. 5, 2019, pp. 1–17.

[155] Boumerzoug, Z. and Y. Helal. Friction stir welding of dissimilar materials aluminum AL6061-T6 to ultra low carbon steel. *Metals*, Vol. 7, No. 2, 2017, pp. 1–9.

[156] Zhang, X., L. Yan, Z. Li, X. Li, G. Gao, H. Yan, et al. Effects of Cu Addition on Age Hardening Behavior and Mechanical Properties of High-Strength Al-1.2 Mg-1.2 Si Alloy. *Materials*, Vol. 16, No. 8, 2023 Apr, id. 3126.

[157] Lin, J. Y., S. Nambu, and T. Koseki. Interfacial phenomena during ultrasonic welding of ultra-low-carbon steel and pure Ti. *Scripta Materialia*, Vol. 178, 2020, pp. 218–222.

[158] Wang, K., K. Zhao, J. Liu, D. Liu, T. Li, W. Li, et al. Interplay of microstructure and mechanical properties of WC-6Co cemented carbides by hot oscillating pressing method. *Ceramics International*, Vol. 47, No. 14, 2021, pp. 20731–20735.

[159] Khan, H. A., J. Li, and C. Shao. Analyses of friction stir riveting processes: A review . *Journal of Manufacturing Science and Engineering, Transactions of the ASME*, Vol. 139, No. 9, 2017, pp. 1–12.

[160] Zhao, D., D. Ren, K. Zhao, P. Sun, X. Guo, and L. Liu. Ultrasonic welding of magnesium–titanium dissimilar metals: A study on thermo-mechanical analyses of welding process by experimentation and finite element method. *Chinese Journal of Mechanical Engineering (English Edition)*, Vol. 32, No. 1, 2019, pp. 1–11.

[161] Chao, Y. J., X. Qi, and W. Tang. Heat transfer in friction stir welding - experimental and numerical studies. *Journal of Manufacturing Science and Engineering*, Vol. 125, No. 1, 2003, pp. 138–145.

[162] Tsiangou, E., S. T. de Freitas, I. F. Villegas, and R. Benedictus. Investigation on energy director-less ultrasonic welding of polyetherimide (PEI)- to epoxy-based composites. *Composites Part B: Engineering*, Vol. 173, February 2019, id. 107014.

[163] Pal, D., N. Hasan, and P. V. Rao. Temperature distribution analysis of Cu, Al and steel material heat exchangers by ANSYS. *Materials Today: Proceedings*, Vol. 56, 2022, pp. 3176–3185.

[164] Musa, M. A., W. A. Wan Saidin, N. I. Kasim, M. I. Ibrahim, and N. Mohamad Noor. A review on ultrasonic welding capability: Breakaway from traditional plastic. *Applied Mechanics and Materials*, Vol. 789–790, June 2015, pp. 136–140.

[165] Wolcott, P. J., N. Sridharan, S. S. Babu, A. Miriyev, N. Frage, and M. J. Dapino. Characterisation of Al–Ti dissimilar material joints fabricated using ultrasonic additive manufacturing. *Science and Technology of Welding and Joining*, Vol. 21, No. 2, 2016, pp. 114–123.

[166] Grabalosa, J., I. Ferrer, O. Martínez-Romero, A. Elías-Zúñiga, X. Plantá, and F. Rivillas. Assessing a stepped sonotrode in ultrasonic molding technology. *Journal of Materials Processing Technology*, Vol. 229, 2016, pp. 687–696.

[167] Carboni, M. Failure analysis of two aluminium alloy sonotrodes for ultrasonic plastic welding. *International Journal of Fatigue*, Vol. 60, 2014, pp. 110–120.

[168] Lun, Z., W. Shicheng, L. Jiguang, Z. Abbas, and X. Gang. Performance enhancement of clinched joints with ultrasonic welding for similar and dissimilar sheet metals. *Welding in the World*, Vol. 67, 2023, pp. 2715–2729.

[169] Tan, M., C. S. Wu, and H. Su. Ultrasonic effects on microstructures and mechanical properties of friction stir weld joints of dissimilar AA2024/AZ31B alloys. *Welding in the World*, Vol. 67, No. 2, 2023, pp. 373–384.

[170] Ao, S. S., M. P. Cheng, W. Zhang, J. P. Oliveira, S. M. Manladan, Z. Zeng, et al. Microstructure and mechanical properties of dissimilar NiTi and 304 stainless steel joints produced by ultrasonic welding. *Ultrasonics*, Vol. 121, No. December 2021, 2022, pp. 1–10.

[171] Lv, X., C. S. Wu, and Z. Sun. Effects of ultrasonic vibration on material flow and thermal cycles in friction stir welding of dissimilar Al/Mg alloys. *Metallurgical and Materials Transactions A: Physical Metallurgy and Materials Science*, Vol. 53, No. 4, 2022, pp. 1572–1584.

[172] Abdi Behnagh, R., P. Esmaeilzadeh, and M. Agha Mohammad Pour. Simulation of ultrasonic welding of Al-Cu dissimilar metals for battery joining. *Advanced Design and Manufacturing Technology*, Vol. 13, No. 2, 2020, pp. 23–31.

[173] Du, P., W. Chen, J. Deng, K. Li, and Y. Liu. Effects of knurl tooth angle on mechanical and thermal behaviors of aluminum ultrasonic welding. *Ultrasonics*, Vol. 108, April 2020, id. 106207.

[174] Huang, H., J. Chen, Y. C. Lim, X. Hu, J. Cheng, Z. Feng, et al. Heat generation and deformation in ultrasonic welding of magnesium alloy AZ31. *Journal of Materials Processing Technology*, Vol. 272, May 2019, pp. 125–136.

[175] Yang, F., J. Zhou, and R. Ding. Ultrasonic vibration assisted tungsten inert gas welding of dissimilar magnesium alloys. *Journal of Materials Science and Technology*, Vol. 3412, 2018, pp. 2240–2245.

[176] Gu, X., C. Sui, J. Liu, D. Li, Z. Meng, and K. Zhu. Microstructure and mechanical properties of Mg/Al joints welded by ultrasonic spot welding with Zn interlayer. *Materials and Design*, Vol. 181, 2019, id. 108103.

[177] Kumar, S., C. S. Wu, S. Zhen, and W. Ding. Effect of ultrasonic vibration on welding load, macrostructure, and mechanical properties of al/mg alloy joints fabricated by friction stir lap welding. *International Journal of Advanced Manufacturing Technology*, Vol. 100, No. 5–8, 2019, pp. 1787–1799.

[178] Jedrasiak, P. and H. R. Shercliff. Finite element analysis of heat generation in dissimilar alloy ultrasonic welding. *Materials and Design*, Vol. 158, 2018, pp. 184–197.

[179] Patel, D. S., A. Singh, K. Balani, and J. Ramkumar. Topographical effects of laser surface texturing on various time-dependent wetting regimes in Ti6Al4V. *Surface and Coatings Technology*, Vol. 349, February 2018, pp. 816–829.

[180] Komiyama, K., T. Sasaki, and Y. Watanabe. Effect of tool edge geometry in ultrasonic welding. *Journal of Materials Processing Technology*, Vol. 229, 2016, pp. 714–721.

[181] Zhang, S., X. Chen, Z. Moumni, and Y. He. Thermal effects on high-frequency magnetic-field-induced martensite reorientation in ferromagnetic shape memory alloys: An experimental and theoretical investigation. *International Journal of Plasticity*, Vol. 108, April 2018, pp. 1–20.

[182] Shakil, M., N. H. Tariq, M. Ahmad, M. A. Choudhary, J. I. Akhter, and S. S. Babu. Effect of ultrasonic welding parameters on microstructure and mechanical properties of dissimilar joints. *Materials and Design*, Vol. 55, 2014, pp. 263–273.

[183] Lee, D., E. Kannatey-Asibu, and W. Cai. Ultrasonic welding simulations for multiple layers of lithium-ion battery tabs. *Journal of Manufacturing Science and Engineering*, Vol. 135, No. 6, 2013, pp. 1–14.

[184] Panteli, A., J. D. Robson, I. Brough, and P. B. Prangnell. The effect of high strain rate deformation on intermetallic reaction during ultrasonic welding aluminium to magnesium. *Materials Science and Engineering A*, Vol. 556, 2012, pp. 31–42.

[185] Hajjari, E., M. Divandari, S. H. Razavi, S. M. Emami, T. Homma, and S. Kamado. Dissimilar joining of Al/Mg light metals by compound casting process. *Journal of Materials Science*, Vol. 46, No. 20, 2011, pp. 6491–6499.

[186] Faudree, M. C., H. T. Uchida, H. Kimura, S. Kaneko, M. Salvia, and Y. Nishi. Advances in titanium/polymer hybrid joints by carbon

fiber plug insert: current status and review. *Materials*, Vol. 15, No. 9, 2022, pp. 1–19.
[187] Zeng, L., B. Wang, X. Liu, J. Wu, L. Deng, M. Yuan, et al. High-resolution air-coupled laser ultrasound imaging of microstructure and defects in braided CFRP. *Composites Communications*, Vol. 28, October 2021, pp. 1–7.
[188] Lionetto, F., F. Balle, and A. Maffezzoli. Hybrid ultrasonic spot welding of aluminum to carbon fiber reinforced epoxy composites. *Journal of Materials Processing Technology*, Vol. 247, May 2017, pp. 289–295.
[189] Dou, G. and A. S. Holmes. System integration for plastic electronics using room-temperature ultrasonic welding. *Advanced Engineering Materials*, Vol. 22, No. 5, 2020, pp. 1–6.
[190] Staab, F. and F. Balle. Ultrasonic torsion welding of ageing-resistant Al/CFRP Joints: properties, microstructure and joint formation. *Ultrasonics*, Vol. 93, No. September 2018, 2019, pp. 139–144.
[191] Li, G., J. Zhao, J. Y. H. Fuh, W. Wu, J. Jiang, T. Wang, et al. Experiments on the ultrasonic bonding additive manufacturing of metallic glass and crystalline metal composite. *Materials*, Vol. 12, No. 18, 2019, pp. 1–11.
[192] Lionetto, F., C. Mele, P. Leo, S. D'Ostuni, F. Balle, and A. Maffezzoli. Ultrasonic Spot welding of carbon fiber reinforced epoxy composites to aluminum: Mechanical and electrochemical characterization. *Composites Part B: Engineering*, Vol. 144, 2018, pp. 134–142.
[193] Yeh, R. Y. and R. Q. Hsu. Development of ultrasonic direct joining of thermoplastic to laser structured metal. *International Journal of Adhesion and Adhesives*, Vol. 65, 2016, pp. 28–32.
[194] Levy, A., S. Le Corre, and I. Fernandez Villegas. Modeling of the heating phenomena in ultrasonic welding of thermoplastic composites with flat energy directors. *Journal of Materials Processing Technology*, Vol. 214, No. 7, 2014, pp. 1361–1371.